

# A Critical Review of Limitations and Challenges in Advancement of HNF as a Green Oxidizer for Composite Solid Propellant Formulations

Bansal, Lakshay; Jindal, Prakhar; Kumar Rathi, Vineet

DOI

10.1002/prep.12072

**Publication date** 

**Document Version** Final published version

Published in

Propellants, Explosives, Pyrotechnics

Citation (APA)

Bansal, L., Jindal, P., & Kumar Rathi, V. (2025). A Critical Review of Limitations and Challenges in Advancement of HNF as a Green Oxidizer for Composite Solid Propellant Formulations. *Propellants,* Explosives, Pyrotechnics, 50(7), 11-30. https://doi.org/10.1002/prep.12072

Important note

To cite this publication, please use the final published version (if applicable). Please check the document version above.

Copyright

Other than for strictly personal use, it is not permitted to download, forward or distribute the text or part of it, without the consent of the author(s) and/or copyright holder(s), unless the work is under an open content license such as Creative Commons.

Please contact us and provide details if you believe this document breaches copyrights. We will remove access to the work immediately and investigate your claim.









# A Critical Review of Limitations and Challenges in Advancement of HNF as a Green Oxidizer for Composite Solid Propellant Formulations

Lakshay Bansal<sup>1</sup> | Prakhar Jindal<sup>2</sup> | Vineet Kumar Rathi<sup>3</sup>

<sup>1</sup>School of Chemical Sciences, University of Illinois, Urbana Champaign, Champaign, Illinois, USA | <sup>2</sup>Marie Sklodowska-Curie Postdoctoral Fellow, Space System Engineering, TU Delft, Delft, the Netherlands | <sup>3</sup>Department of Chemical and Materials Engineering, New Jersey Institute of Technology, Newark, New Jersey, USA

Correspondence: Prakhar Jindal (p.jindal@tudelft.nl)

**Keywords:** ammonium nitrate | ammonium perchlorate | composite solid propellant | energetic binders | green energetic materials | green oxidizers | hydrazinium nitroformate

#### **ABSTRACT**

Hydrazinium nitroformate (HNF) is a chlorine-free, high-energy oxidizer with promising applications in green propulsion systems. This review examines the thermal decomposition, combustion kinetics, flame structure, and behavior of HNF, while critically evaluating the current body of literature. Thermal studies reveal that HNF undergoes two-stage decomposition, with exothermic peaks at 136°C and 138°C and an activation energy of 150 kJ/mol, determined using Kissinger and Ozawa methods. The decomposition products include nitroform, hydrazine, and nitrogen oxides, with a 72.5% weight loss in the first stage (105°C–142°C) and 24.5% in the second stage (142°C–210°C). Combustion studies identify a three-zone flame structure: fizz zone, dark zone, and luminous flame zone, with temperatures ranging from 1320 to 1540 K near the surface to 2720 K in the outer flame. HNF exhibits a high-pressure exponent (~0.85), necessitating optimization through burn rate modifiers (BRMs) and advanced formulations. While HNF demonstrates superior specific impulse and reduced exhaust plume radiation compared to ammonium perchlorate (AP), its needle-like crystal morphology poses challenges for handling and propellant integration. This review emphasizes the need for advanced diagnostic techniques, computational modeling, and innovative BRMs, along with polymeric binders that are compatible with HNF and can improve the performance of HNF-based systems, offering valuable insights for green propellant development.

## 1 | Introduction

High-pressure, high-enthalpy gaseous products from exothermic chemical reactions are expanded through a nozzle to generate the forward motion of the rockets. The combustion reaction between the fuel and the oxidizer generates heat energy due to the formation of new and stronger bonds between the electronegative oxygen atom and the fuel producing these high-energy gases [1–3]. A composite solid propellant (CSP) formulation consisting of aluminum (Al) powder as the metallic fuel, ammonium perchlorate (AP; NH<sub>4</sub>ClO<sub>4</sub>) as the oxidizer and a polymeric

binder such as hydroxyl-terminated polybutadiene (HTPB) or polybutadiene acrylonitrile (PBAN) is often used by the various space agencies around the globe, particularly in the first stage of the rockets [4–7]. Various other combinations of different fuels and oxidizers, such as magnesium (Mg) powder and ammonium nitrate (AN) (NH $_4$ NO $_3$ ), sugar, potassium nitrate (PN; KNO $_3$ ), and so forth, are available. Low combustion performance constrains the extended use of the combination of magnesium and AN for commercial rocket applications and is often used for amateur rocketry [8–11]. AP is a high-density compound with an oxygen balance (OB) of  $\sim$ 34% and is extensively used as an oxidizer

This is an open access article under the terms of the Creative Commons Attribution License, which permits use, distribution and reproduction in any medium, provided the original work is properly cited.

© 2025 The Author(s). Propellants, Explosives, Pyrotechnics published by Wiley-VCH GmbH.

because of its excellent performance and ballistic properties [12]. Aluminum powder is preferred as the fuel with AP due to high volumetric and gravimetric energy densities, the catalytic effect of nano-sized Al particles on the decomposition of AP, and its ability to produce a very high-temperature flame, which together leads to the high specific impulse of the CSP grain [13–17].

#### 1.1 | Solid Oxidizers

The oxidizer is the major constituent of any CSP composition as it tends to occupy around 70%–85% of the weight of the composition [18, 19]. High positive OB, high heat of formation, and high thermal stability are some of the important characteristics of an oxidizer [20]. Equation (1) represents the formula to obtain OB for a compound where *X* represents the number of carbon atoms in the compound, *Y* represents the number of hydrogen atoms in the compound, and *Z* represents the number of oxygen atoms in the compound [21].

OB% = 
$$\frac{-1600}{\text{molar wt.}} \times [2X + (Y/2) - Z]$$
 (1)

Perchlorate and nitrate salts of the inorganic compounds such as ammonium and metallic elements (alkali or alkaline earth metals) such as potassium are the mostly used oxidizers for the formulation of CSP grains [22, 23]. PN, an inexpensive solid oxidizer with low hygroscopicity, is widely used in pyrotechnics and explosives, especially in black powder, due to its ability to oxidize carbon exothermically. Although it has high endothermic decomposition, making it suitable for use with highly energetic fuels, it is not preferred in commercial propellants [24-26]. Potassium perchlorate (PP), often used in pyrotechnic formulations, has high decomposition temperatures and poor reactivity with organic matter. However, its enhanced versions with nano-metals and various other perovskites are being studied for better ignition and energy release mechanisms along with countering its hygroscopicity which can negatively affect nanosized fuel particles and propellant stability [27, 28]. AN, used in secondary explosives, has limitations due to its phase transitions at room temperature, which lead to volume instability and crack formation in propellant grains. Despite its potential as a green solid oxidizer, it is not widely used in commercial rockets [29-32]. Conclusively, due to their low combustion performance as compared to AP, salts of potassium such as PN and PP (KClO<sub>4</sub>) find their applications in the formulation of pyrotechnic igniters [33].

AP, known for its high thermal stability and complete gaseous decomposition above  $300^{\circ}$ C, is the preferred oxidizer in many solid propellants. Its burn rate can be enhanced by adding metallic oxides like Fe<sub>2</sub>O<sub>3</sub>, CuO, and NiO, which catalyze its decomposition and improve oxygen release [35–38]. Figure 1 represents the DSC curve, which reflects two distinct decomposition stages of AP [34]. Table 1 presents the various important properties of some conventional solid oxidizers of interest.

Other oxidizers include nitrate salts of sodium, barium, and strontium, as well as the compounds of chlorate, permanganate, dichromate, and peroxides. Because of the inferior stability, ignition, and performance characteristics, these oxidizers are

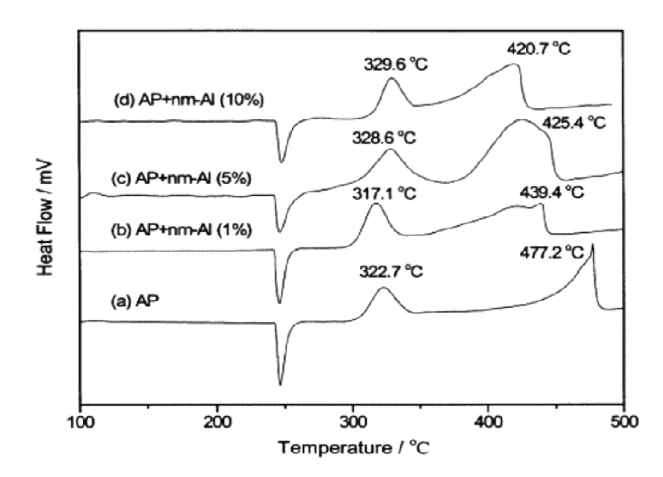


**FIGURE 1** | DSC curve of pure AP [34].

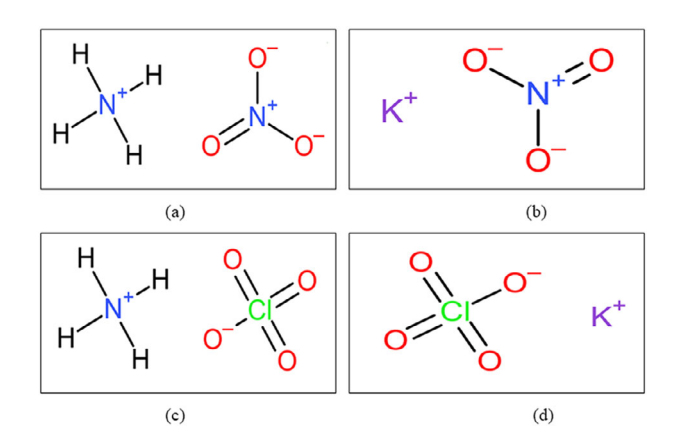


**FIGURE 2** | Ionic form structures of (a) ammonium nitrate, (b) potassium nitrate, (c) ammonium perchlorate, and (d) potassium perchlorate.

not preferred for the formulation of CSP grains. However, these oxidizers tend to find their applications in small-scale pyrotechnics because of their peculiar characteristics, such as colored flame and delay composition [43]. Figure 2 represents the ionic structure of different conventional solid oxidizers used in CSP formulations and other pyrotechnic applications.

## 1.1.1 | Negative Impacts of Conventional Solid Oxidizers

Thermal decomposition products of AP include  $O_2$ , HCl,  $N_2$ ,  $N_2$ O, HClO<sub>4</sub>, NOCl, H<sub>2</sub>O, and Cl<sub>2</sub> as is represented in Equation (2). Oxygen and HCl are the products of prime interest here as to where the free oxygen is necessary for the combustion of fuel, gaseous HCl produces hydrochloric acid interacting with H<sub>2</sub>O and results in acid rain [12, 44]. Other than increasing the acidity of the rain, HCl emissions significantly affect the pH level of the soil.

$$10NH_4ClO_4 \rightarrow 2.5Cl_2 + 2N_2O + 2.5NOCl + HClO_4 + 1.5HCl + 18.75H_2O + 1.75N_2 + 6.375O_2$$
 (2)

Furthermore, HCl breaks down into free radicals of chlorine and reacts with ozone in the atmosphere, thereby depleting

**TABLE 1** Different properties of oxidizers of major interest.

Compound	Chemical formula		Oxygen balance (%)	Molar mass (g/mol)	Boiling point (°C)	Melting point (°C)	Heat of formation (kJ/mol)	References
AP	NH <sub>4</sub> ClO <sub>4</sub>	1.950	27.23	117.49	_	130	-296.00	[37]
AN	$NH_4NO_3$	1.725	20.00	80.043	210	169.9	-367.50	[32, 39]
PP	$KClO_4$	2.520	46.20	138.55	600	525	-430.12	[40]
PN	$KNO_3$	2.110	47.47	101.10	400	333	-494.60	[41, 42]

the ozone content of the layer. The reaction between the free radicals of chlorine and ozone produces oxygen as represented in Equation (3) [44, 45].

$$Cl \cdot +O_3 \rightarrow ClO \cdot +O_2$$
 (3)

The fact that CO<sub>2</sub> and CO are the major air pollutants can also not be neglected. Ammonium and nitrate-based oxidizers liberate NO2, NO, and so forth upon their decomposition. The emission of nitrous oxide gases not only affects human health but is also a major air pollutant and degrades the water quality by increasing nitrogen loading [46]. Perchlorate is one of the known thyroid disruptors. It competes with the absorption of iodine in the human body, resulting in decreased production of thyroxin and triiodothyronine, thereby triggering the thyroid-stimulating hormone. These hormones are essential for protein absorption and the proper development of immature neurons [47]. Surface and groundwater contamination from the combustion products of perchlorate salts is extensively reported in China, Japan, Korea, India, and the USA. The accumulated perchlorate is absorbed and ingested by wild plants and animal species, including amphibians and fish [48].

### 1.2 | Green Oxidizers

As the number of space missions and rocket launches are seen to increase, there exists a need to find novel and green replacements for current CSPs. The development of eco-friendly and nontoxic oxidizers to be used as the component of CSP grains is of supreme interest. AN shows the capability to replace AP as an eco-friendly alternative, and therefore, several phase-stabilized versions of AN are being developed, researched, and tested, exhibiting reduced or almost no signs of polymorphism. Organic compounds such as polyvinyl pyrrolidine, polyethylene glycol, and polyacrylamide have been added to the crystal lattice of AN, resulting in an acceptable percentage of phase stabilization in AN [49]. The different weight percent of inorganic compounds like KNO<sub>3</sub> and CsNO<sub>3</sub> have been used to enhance the stability of different AN phases [50]. Oxides and diamines of metals like copper, nickel, and zinc have also been used to achieve phase stabilization [51].

Many other eco-friendly solid propellant ingredients such as hydrazinium nitroformate (HNF), ADN, FOX-7, GAP, dinitrourea, BAMO, CL-20, and so forth are being synthesized and tested by researchers [52–58]. Along with inventing new energetic compounds, researchers are also producing various derivatives by replacing and/or adding different functional groups or elements in the existing compounds [59, 60].

#### 1.2.1 | Need for Green Oxidizers

Numerous organizations have raised concerns about the impact of hazardous exhaust gases from rocket launches and their effects on the local and global environmental conditions of the planet. The depletion of ozone content in the stratosphere is indeed resulting in climate change and, hence, is a matter of global concern [61, 62]. This concern has taken a fast pace in the last two decades, and thus, a large number of researchers are extensively working toward finding eco-friendly or green alternatives to existing oxidizers with comparable performance characteristics.

#### 1.2.2 | Benefits of Green Oxidizers

The extensive use of green oxidizers in CSP grain formulations delivers numerous crucial direct and indirect benefits in many aspects of commercial rocket applications, such as biological, ecological, economic, and so forth. No release of free halogen radicals can directly eliminate the negative impact on the biotic and abiotic components of the ecosystem [63]. There can be a significant reduction in the acidity level around the launch site as well as that of nearby water reserves [64]. There can be negligible acid production in the atmosphere as the exhaust from the combustion of eco-friendly oxidizers is completely halogen-free [44].

Stainless steel and aluminum are the most used metals in the construction of the supporting structures at the launch site which tend to corrode in a moist environment having chlorine gas available in abundance [65]. It is a well-known fact that the free radicals are of much greater reactivity. On being expelled from the nozzle, free radicals of chlorine tend to react with the nearby infrastructures, thereby changing the mechanical properties of the structures [66]. The chlorine-free exhaust, however, does not degrade the structural integrity of the supporting infrastructure of the launch pad. This tends to result in increased service life and cost-effectiveness of the launch systems. Also, green oxidizers with no free halogen radicals produce less dense exhaust when compared to the exhaust of conventional oxidizers that include free radicles of halogens. The use of green oxidizers tends to result in quick dispersion of the exhaust plume or even the production of no trailing exhaust plume, which facilitates the non-detectable operation of missiles and security of the location of the launch site. This property is extensively sought out, particularly for defense applications. The chlorine-free exhaust tends to mitigate the problems of local and global depletion of the stratospheric ozone. Green oxidizers do not have any such element in their chemical structure that may harm the integrity of the ozone layer

**TABLE 2** | Properties of hydrazinium nitroformate [68–71].

Property	
Chemical formula	$CH_5N_5O_6$
Density	$1.86 \text{ g/cm}^3$
Oxygen balance	13.10%
Molar mass	183.08 g/mol
Melting point	121°C-125°C
Heat of formation	−72 kJ/mol
Heat of evaporation	164.8 kJ/mol

upon their release after combustion. Thus, it is safe to say that the use of green oxidizers tends to deliver numerous significant advantages over conventional oxidizers.

The novel aspects of this work lie in its comprehensive analysis of HNF combustion and thermal behavior, synthesizing insights from various studies to provide a clearer understanding of this promising oxidizer. To the best of the author's knowledge, no comprehensive study is available that reports the important aspects combined in a single document of such a novel green oxidizer to be used in CSP grain formulations. The present study aims to provide a detailed review of the studies carried out on the various crucial aspects of HNF, that is, benefits, different synthesis routes, and structural, chemical, mechanical, and combustion properties of HNF as the green oxidizer. By identifying gaps in current research, this review offers valuable directions for future investigations, including the development of advanced diagnostic techniques, computational models, and optimized BRMs. For the researchers exploring green propellants, this review underscores the importance of addressing thermal decomposition challenges, pressure-dependent characteristics, and compatibility issues in HNF-based formulations.

## 2 | HNF as a Novel Green Oxidizer

HNF ( $\mathrm{CH_5N_5O_6}$ ) is a yellow-colored salt of hydrazine (HZN) ( $\mathrm{H_2N_4}$ ) and nitroform (NF) ( $\mathrm{HC(NO_2)_3}$ ) with a needle-like crystal shape. HNF is also known as hydrazine trinitromethane. From the rocket propulsion viewpoint, it is a chlorine-free, high-energy, high-density, solid oxidizer with a low signature exhaust trail. Large heat of formation and powerful exothermic combustion reaction of HNF leads to a high specific impulse ( $I_{\mathrm{sp}}$ ) and an elevated burn rate [39, 67]. Along with the mentioned properties, HNF, with low hygroscopicity and acceptable thermal stability as additional benefits, can contribute to the easy castability of thixotropic propellant compositions [68]. Various physiochemical properties of HNF are mentioned in Table 2.

Discovered in 1951, most of the experiments and research focused on discovering various safe methods to synthesize HNF and control the particle size. Exploration of HNF was ceased due to two main reasons, hazardous synthesis process and incompatibility with extensively used conventional binders like HTPB, back then. In 1987, the European Space Agency and the Netherlands Agency for Aerospace Programs again started the research on HNF in

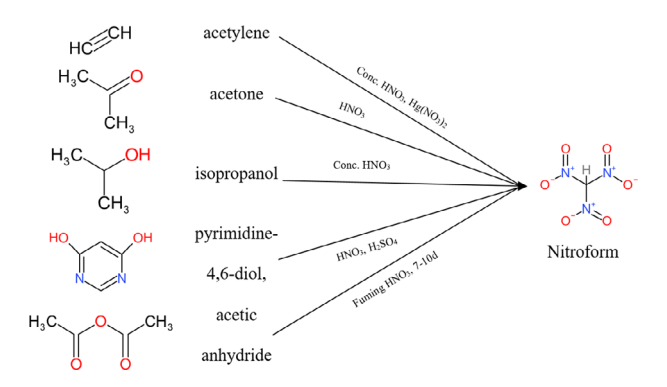


FIGURE 3 | Various substrates used for nitroform synthesis.

persuade to develop high energy halogen-free energetic material [72, 73].

Liquid HNF and HNF solutions with water and methanol as solvents are also being tested to be used as liquid propellants. Some experiments suggest that the combination of HNF and water can replace HZN for application in monopropellant thrusters to control the satellite attitude, but extensive use is restricted by low solubility [74, 75]. Similarly, deploying a combination of HNF dissolved in water and lower alkanols like ethanol or methanol as fuel has been proposed by Van den Berg et al., as the replacement of HZN would result in a safer and simpler mission with reduced cost for the overall project [76]. It was found in a study that the catalytic ignition for liquid monopropellant obtained by dissolving HNF in water, gave promising results when Shell 405 (33% iridium on Al<sub>2</sub>O<sub>3</sub>) was used as the catalyst [77].

#### 2.1 | Chemistry of Synthesis Routes and Structure

Hydrazine nitroformate (HNF) is a salt that contains HZN and NF. The process of producing HNF involves two main steps. First, a precursor is nitrated to produce NF, which is then used to make HNF. Nitroform (NF) itself is a brown, toxic, and volatile liquid when at room temperature. To create HNF, it is crucial to first synthesize NF.

## 2.1.1 | Synthesis of NF

The synthesis of NF has historically been a challenging task. Initially, it was synthesized by nitrating acetylene gas to tetranitromethane (TNM), which was then converted to NF using KOH and  $\rm H_2SO_4$ . Also, Hatan's method involves nitration of acetic anhydride [78]. However, these methods had several drawbacks, including high heat generation, the hazardous nature of the intermediate, potassium nitroformate (KNF), and the low yield of NF. Welch et al. [79] came up with a technique in 1970 that involved using acetone and 90%  $\rm HNO_3$ . However, this method had certain risks associated with it because acetone is volatile and flammable.

NF was produced by utilizing various precursors, including acetylene, acetone, 4,6-dihydroxy pyrimidine [80], isopropanol [81], and acetic anhydride, as shown in Figure 3. Because of

**TABLE 3** Nitroform yield produced from isopropanol from various nitrating methods.

Substrate	Nitrating agent	Time	Molar ratio (nitric acid to isopropyl)	Yield	
H <sub>3</sub> C OH	98% Conc. HNO <sub>3</sub>	2-4 h	10:1 to 25:1	25%	
	Fuming HNO <sub>3</sub>	3h	12:1 to 15:1	51.3%	
CH <sub>3</sub>	Anhydrous HNO <sub>3</sub>	1–2 h	14:1	53.6%	

isopropanol

intrinsic difficulties in current synthetic methods, commercial NF synthesis lags far behind laboratory research. These include safety issues associated with the acetylene route, high costs linked to the pyrimidine-4,6-diol method, and hazardous procedures for the environment that use acetic anhydride as a substrate.

2.1.1.1 | Synthesis of NF From Isopropanol. When it comes to NF synthesis, isopropanol has several benefits over other substrates, including affordability, safety, and environmental friendliness. Therefore, for large-scale production, the synthetic pathway from isopropanol may be intriguing. Before 1978, the production of NF from the reaction mixture involved a hazardous technique known as vacuum distillation. This technique was dangerous due to NF's formation of an azeotropic mixture with nitric acid. Separation of the mixture required high temperatures, which posed a risk of explosion. As a result, the development of high-purity nitrogen trifluoride as a crucial oxidizer faced slow progress. Another method that utilizes isopropanol and conc. HNO<sub>3</sub>, as a nitrating agent, is considered safer and yields a 25% product, making it a promising alternative [78]. It was challenging to conduct further studies on the optimal reaction parameters for enhancing the yield of NF from isopropanol. However, the possibility of conducting further research appeared to be difficult to ascertain. Furthermore, the challenge of getting pure NF made NF measurement tricky. Moreover, no prior research has addressed the mechanism for NF synthesis from isopropanol, even though it is essential for increasing the yield of target compounds.

Anhydrous HNO<sub>3</sub> and fuming nitric acid were used as nitrating agents in a work by Ding et al. [82, 83] to create NF from isopropanol. To get the maximum NF yield possible, they adjusted the nitrating agent's molar ratio and reaction time, optimizing the reaction conditions. Fuming HNO<sub>3</sub> showed good efficiency in the manufacture of NF using a gentle, effective, and time-saving nitration process. Anhydrous HNO<sub>3</sub> showed superior nitration capability without sacrificing oxidation capacity when compared to fuming HNO<sub>3</sub>. The NF yield achieved in both cases was more than double that reported by Frankel [81]. Table 3 represents different nitration methods that are used to synthesize NF from isopropanol as a precursor.

**2.1.1.2** | Other Methods to Synthesize NF. Lu et al. [84] proposed a cost-effective method for synthesizing NF in a research study. According to the study, NF can be produced by nitrolyzing cucurbituril (CB) using a mixed solution of acetic anhydride in fuming nitric acid, as presented in Figure 4. The high symmetry and rigid structure of CB make it an ideal candidate for this process [6]. This new nitration method is considered to be mild and safer, providing a safer and less risky reaction condition for the synthesis of NF.

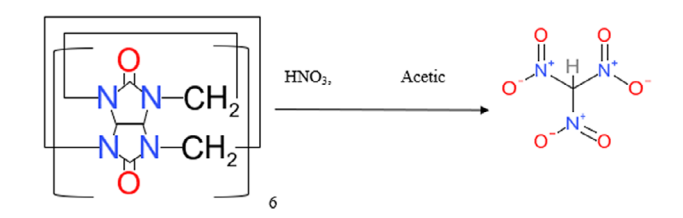


FIGURE 4 | Nitrolysis of cucurbituril CB 6 to produce NF.

**FIGURE 5** | NF synthesis mechanism using acetylacetone.

An investigation by Yan et al. [85] focused on the synthesis of NF from  $\alpha\text{-methyl}$  carbonyl derivatives, specifically acetylacetone. The reaction for this synthesis technique is presented in Figure 5. They discovered that the use of acetic anhydride in fuming nitric acid was an effective method for producing NF from acetylacetone. By optimizing their approach with a 200:1 molar ratio of fuming nitric acid to acetic anhydride at 60°C, they were able to obtain pure NF at 40.8% yield. This method provides an affordable, mild reaction condition and satisfactory yield, making it a promising and cost-effective alternative route for industrial NF production.

## 2.1.2 | HZN Production

HZN was first introduced on an industrial scale by Rasching [86] in 1907 through a process that involved the reaction of ammonia with sodium hypochlorite to produce monochloramine, which then further reacted with ammonia to yield HZN. In 1937, urea was used as a substitute for ammonia in this reaction by Otto Seuffert and Egon Ihwe [87]. This was followed by Bayer's ketazine [88] process in the 1950s, which utilized sodium hypochlorite in the presence of acetone to oxidize ammonia, leading to the formation of ketazine that is subsequently hydrolyzed to produce HZN. All these traditional methods employed chlorinebased oxidation. The most recent synthesis of HZN utilizes a chlorine-free process that uses hydrogen peroxide as an oxidizing agent to oxidize ketone-ammonia systems in the presence of nitriles, resulting in the production of azines through oxaziridine intermediates. This innovative approach significantly reduces chloride waste and enhances environmental sustainability [89].

As a result of these advancements, HZN is readily available on an industrial scale today, providing a consistent precursor for subsequent reactions, such as the acid-base synthesis of HNF, where the main challenge has shifted to the synthesis and handling of NF instead of HZN itself. The following section will focus on the synthesis of NF, followed by the synthesis of HNF.

#### 2.1.3 | Synthesis of HNF Using NF

The manufacturing process of HNF involves a direct acid-base reaction between NF and HZN. However, it is imperative to handle the raw materials with utmost care due to their hazardous properties, which include toxicity, carcinogenicity, reactivity, and explosiveness. Even slight contamination of these ingredients can lead to compromised quality of HNF due to unwanted side reactions or interactions with impurities during the production process. Also, maintaining the precise stoichiometric ratio between the two raw materials is crucial, as any deviations can result in the rapid deterioration of the HNF product. Therefore, implementing stringent quality control measures for both the ingredients and the manufacturing process is essential to ensure the consistent production of high-quality and stable HNF. These measures are vital to minimize risks and guarantee the safety and efficacy of the final product.

The synthesis of NF was conducted based on the methodologies outlined in Frankel et al.'s [81] studies, followed by its conversion to HNF using the procedures detailed by Lovett and Edison [69]. Their method involves mixing NF and anhydrous HZN in equimolar amounts in an organic solvent like methanol at atmospheric pressure and 0°C-50°C. Researchers at Prins Maurits Laboratory, TNO Netherlands [76], have developed a reliable and secure method for synthesizing HNF from NF. High-purity HZN and NF in a Dichloroethane solvent at 0°C-5°C. The coarse HNF obtained after drying was then recrystallized using a nonsolvent methylene chloride and methanol as solvent. The process started at the lab scale and yielded 10 g per batch. It was then upscaled to 300 g per batch. The process of crystallization plays a crucial role in the formation of HNF. Later, Veltmans et al. [90] synthesized HNF by employing ultrasonic vibration at 20 kHz for crystallization. The HNF obtained through this method demonstrated higher stability compared to the conventional method that did not use ultrasonic vibration.

Schoyer et al. [91] devised a method for producing HNF by extracting NF from an aqueous phase into ethylene dichloride (EDC) with the aid of sodium chloride. HZN was then introduced into the NF/EDC solution. The resulting HNF/EDC mixture underwent filtration and washing stages to eliminate impurities. Finally, the HNF crystals were subjected to drying in a vacuum oven under controlled temperature and pressure conditions to ensure the stability and quality of the product.

$$N_2H_4(l) + HC(NO_2)_3(l) \rightarrow N_2H_5^+ + C(NO_2)_3^-(s)$$
 (4)

Jadhav et al. [92] introduced two new derivatives of HNF called monomethyl and dimethyl HNF. Different derivatives, along with their structures, are illustrated in Table 4. Initially, NF was synthesized by using sulfuric acid and fuming nitric acid as a nitrating system for isopropanol. The HZN was added to

NF in a dichloroethane solution at 15°C–20°C under a nitrogen environment. The solution was stirred for 2 h, followed by recrystallization using methane. Using methyl HZN and dimethyl HZN solutions in xylene using the same procedure produces MMHNF and DMHNF, respectively. Among these derivatives, HNF demonstrates potential as an environmentally friendly oxidizer, MMHNF shows promise as a high-performance energetic material, and DMHNF appears to be a possible component for creating melt-castable high explosives.

HNF is synthesized using two precursors, which are HZN and NF. HZN is an easily available commercial compound. The schematic to prepare HNF is illustrated through the flow chart in Figure 6.

#### 2.1.4 | Chemical Structure

The main structural focus remains on the anion part of HNF, that is, NF, also called nitroformate. Different compounds can take the place at the cationic site, producing very less difference in the chemical structure properties of the produced NF compound [93]. Figure 7 represents the chemical structure of HNF.

The crystallographic investigation reveals that the crystal particles of HNF are packed in a monoclinic system. The hydrogen bonding between the cation and anions leads to tight packing, resulting in a high density of HNF. As can be seen from the figure, HNF consists of  $N_2H_5^+$  which is staggered in shape and  $C(NO_2)_3^-$  which is elliptical in shape. The C—N bonds are arranged in a trigonal planar structure format with the dihedral angle between  $4^\circ$  and  $74^\circ[68,70]$ .

#### 2.1.5 | Structure and Chemical Bonding of Nitroformate

Dickens conducted an in-depth study to analyze and compare the structure of cyanoformate and nitroformate anions. The study reveals that the structure of the cyano derivative could be planar, whereas a detailed analysis of the nitroformate structure was performed using three-dimensional single crystal XRD. XRD characterization concluded that the anion is precisely propellor-shaped, centered with the carbon atom and three coplanar nitrogen atoms [94]. It is also observed that the C—N bond in the nitroformate ion is nonequivalent. The nitro groups in the ion can also be rotated through different angles about the plane of the C—N bond [95].

In a comparative study between HNF, ammonium nitroformate (ANF), aminotriazole nitroformate (ATNF), and guanidinium nitroformate (GNF), it was found that the h-bond strength of HNF was higher than the others, having a minimum core-valence bifurcation index value of -0.0032 [93].

Quantum theory of atoms in molecules (QTAIM) analysis was performed by Zang et al., to study the intermolecular hydrogen bonding for various compounds including HNF. Presence of two week hydrogen bonds was detected [96]. Equation (5) was used to obtain the values for hydrogen bond energy ( $E_{\rm HB}$ ) using the potential electron energy density ( $V_{\rm CBN}$ ) value obtained by

Monomethlhydrazine nitroformate (MMHNF)

Dimethlhydrazine nitroformate (DMHNF)



FIGURE 6 | Steps to prepare HNF from hydrazine and nitrofrom.

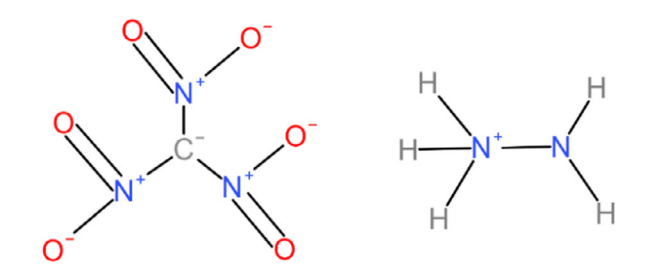


FIGURE 7 | Structure of hydrazinium nitroformate.

QTAIM [97].

$$E_{\rm HB} = \frac{V_{\rm CBN}}{2} \tag{5}$$

The value of  $E_{\rm HB}$  obtained for single H-bond in HNF was  $-8.01~\rm kJ/mol$  and considering the fact that there are two of these bonds, the total value was  $-19.55~\rm kJ/mol$  [96].

## 2.2 | Physical Properties

Various factors affect the physical properties of a chemical compound, such as melting point, density, and crystal structure. The most significant factors are the purity level of the precursors, the kind of impurities, size, and shape of the particles [98]. The choice of anion and cation is a major deciding factor in the case of sensitivity and stability of a compound [99].

## 2.2.1 | Melting Point

Different pieces of literature used different methods to determine the melting point of HNF such as DSC/TGA testing, differential thermal analysis (DTA) testing. This led to a variety of melting point values but all of which are in the temperature range of 115°C–125°C [69, 70, 100]. A value of 124°C was obtained by conducting two different procedures, namely, black body thermocouple measurement and oil bath measurement technique [98].

#### 2.2.2 | Density

There can be seen a range in the density of the compound. This was due to the fact that density directly depends on purity. Determination of density took place over an interval of time and the discovery of advanced techniques and equipment led to an increase in the purity of HNF. The density of this energetic compound was calculated using different methods, such as x-ray diffraction, which gave a value of  $\sim 1.9 \, \text{g/cm}^3 \, [101]$ . Two different pycnometric tests were done using helium and dodecane. The values obtained from these two tests were almost the same, that is,  $\sim 1.869 \, \text{g/cm}^3 \, [102]$ .

#### 2.2.3 | Particle Crystal Structure

It is repeatedly reported that HNF has a sharp and long needle-like particle structure [70]. The length to diameter (L/D) ratio is a crucial factor in determining the various particle shape-dependent characteristics of a compound [103]. Various

and-conditions) on Wiley Online Library for rules of use; OA articles are governed by the applicable Creative Commons License

15214087, 0, Downloaded from https://onlinelibrary.wiley.com/doi/10.1002/prep.12072 by Technical University Delft, Wiley Online Library on [17/07/2025]. See the Terms and Conditions (https://onlinelibrary.wiley.com/erms



**FIGURE 8** | Virgin HNF crystals with sharp edges and corners and very high  $L/D \sim 6.0$  [106].

techniques, such as solvent/nonsolvent (S/NS) recrystallization, the inclusion of crystal shape modifier (CSM), and so forth, are employed to reduce the L/D ratio as well as change the crystal shape of any compatible compound, including HNF [70, 103, 104]. The implication of sonocrystallization has been adopted as a recent alternative to conventional crystallization methods where the particle morphology needs to be transformed. The perturbating effect of electromagnetic waves on the nucleation process of the developing crystal leads to the controlled crystallization process [105]. In the case of restructuring for the HNF crystals, ultrasonic waves are used.

S/NS recrystallization, when performed using methanol/carbon tetrachloride (CTC) and ethanol/CTC, ethanol/CTC gave a better reduction in the L/D ratio with a value of 5.21 compared to 6.47 obtained for the competing composition [106], which is illustrated in Figure 8. The ratio can be reduced further through mechanical stirring, using ultrasonic waves, and the combination of the two methods [107]. It was found that the particles produced through the mechanical stirring were fine and uniform with round edges but the L/D ratio was greater when compared to the particles, which included the use of ultrasonic waves. To counter this, the combination of both methods was employed to obtain round-edged crystal particles with an L/D ratio of 3.4 [106].

In another attempt to modify the morphology of the HNF crystals, Schoöyer et al. tried a special cryogenic crystallization [108]. This method is not only an easy crystallization method for HNF, also it can be used to add burn rate modifiers (BRMs), stabilizers, and also to coat the crystal particles with a protective layer to reduce the chances of the propellant grain degradation, which is discussed in detail in Section 2.4.3. The particle diameter was found to be 10 and 2  $\mu$ m, and between 3.5 and 7  $\mu$ m with L/D ratio of 1, 1, and 2 for neat HNF, HNF with 2% stabilizers, and HNF with 2% coating, respectively [109].

Pressing under a pressure of 4–5.75 MPa has also been used on the particle with an L/D ratio of more than 4 to obtain a

ratio of less than 2.5. Pressing can be combined with mechanical posttreatment techniques to round the sharp edge of the obtained grain [110]. One such technique used is drumming, in which the material to be treated along with very small ceramic balls (with a diameter of about 2 mm) are placed in a cylindrical tube and slowly rotated [110, 111].

Figure 9 represents the HNF crystals obtained through different crystallization techniques. It can be seen that multiple attempts with a variety of different techniques are being employed to obtain a lower L/D ratio for the HNF particles. Different methods with non-interacting behavior with each other can be utilized in a step-by-step manner to reduce the L/D ratio to the request measurements.

### 2.2.4 | Friction and Impact Sensitivity

It is a known fact that the higher the aspect ratio of the compound, higher will be its sensitivity towards friction and impact. In the case of the compound being considered to be used in a propellant composition, it is very crucial for the compound to be insensitive to friction and impact.

Impact sensitivity of contaminated and pure HNF samples were obtained using BAM apparatus. A value of less than 1 N m was obtained for impure sample which was considered unfit to be used for the purpose of propellant. Improved HNF samples were synthesized by recrystallization of contaminated sample, which gave a value of 1.5 N m. With further improvement, impact sensitivity of 3Nm was also obtained. The friction sensitivity of pure HNF was found to be 25 N [98, 112]. A cured grain consisting of 59% HNF, 21% Al, and 20% GAP gave a value of 15 N m and 24 N for impact and friction sensitivity, respectively [98].

Rotter impact testing along with rotatory friction testers are also used to find the sensitivity of the compound. The value for the same are found out to be 33FoI and 1.3–1.5 FoF, along with a value of 80 N m for the friction sensitivity for phlegmating HNF with gel [113].

**2.2.4.1** | **Desensitization.** As discussed previously, various research were conducted to reduce the particle size as well as the L/D ratio. Various techniques such as mechanical crystallization, sonocrystallization, phlegmatization, and so forth have been applied in an attempt to produce round-edged particles thus reducing the sensitivity of the compound [105, 114]. The efforts to modify the particle as well as crystal morphology and features are being made as the friction and impact sensitivity of the oxidizer directly related to these physical factors.

To improve the frictional and impact characteristics of HNF, its particles were coated with HTBP nanocomposite which led to the production of almost spherical crystals. Interestingly, it was seen that the energy-dispersive x-ray spectroscopy (EDS) profile gave a peak for nitrogen elements, too, along with that for carbon and oxygen. This corresponds to the conclusion that the coating done on the particles was insufficient. Thus, the procedure was repeated with coating done in two stages, keeping the quantity same. When the double-coated HNF particles were analyzed for the EDS profile, it was found that there were no peaks for

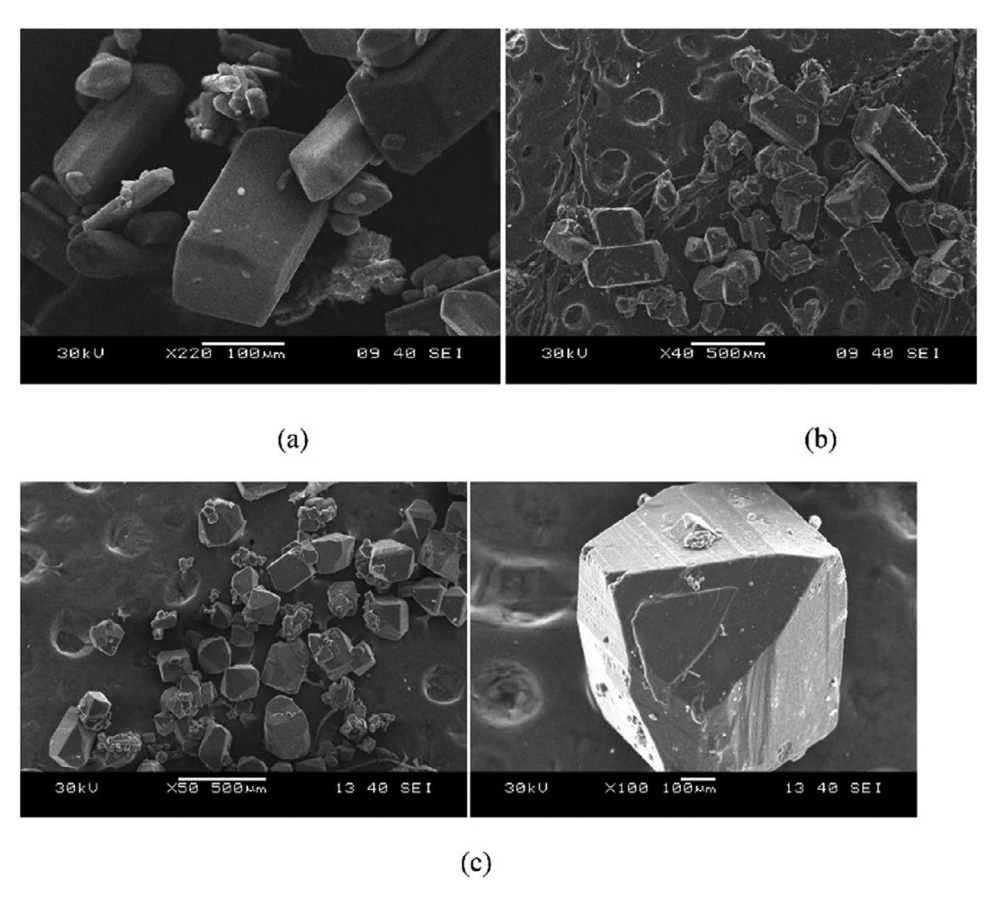


**FIGURE 9** HNF crystals obtained using (a) antisolvent crystallization, (b) sonocrystallization, (c) sequential cooling crystallization. Reprinted (adapted) from [83] with permission from the American Chemical Society).

nitrogen. Due to the smooth surface and facet obtained through the coating process, the benchmark load value for the BAM friction sensitivity test was found to be 9.6 kg [106].

Another crystallization method, namely the sequential cooling crystallization method, was used to obtain an L/D ratio of 1:1. The method consisted of cooling done at a rate of  $-0.3^{\circ}$  C/min. It was found that the particles hence obtained had round and nonpointy edges. Also, when HNF obtained through the sequential cooling method was tested for impact sensitivity, it was found to be the same as that of HMX and AND with a value of 33 cm for the drop hammer test with 2 kg weight [83].

#### 2.2.5 | Stability at Room Temperature

The vacuum thermal stability (VTS) test is a widely used analysis technique to determine the thermal stability of propellants and energetic materials. The value for the compound to be considered thermally stable is when the amount of evolved gas is less than 5 mL/g when kept at 100°C for 48 h [115]. Many researchers working on HNF have used the VTS test to observe the stability of the compounds. However, there was a small disagreement among the results due to the different conditions under which the tests were performed. The VTS test for HNF is most often performed at 60°C because the melting point of HNF is around 120°C. The melting point gave a capping limit to the testing temperature range for the VTS test. Thus, it was suggested to

reduce the assessment value of 5 mL/g of gas evolved to < 1 mL/g as the temperature and the heating time of VTS of HNF is reduced [116].

The stability of HNF depends upon many factors, one of which is the purity of HZN being used to manufacture [116, 117]. Gadiot et al. performed a VTS test for HNF at 60°C for 48 h and found that the result values decreased from 3.1 to 1.2 mL/g as the HZN purity/percentage increased from 96.24% to 99.95% [117]. Almost similar results were obtained when the VTS test was performed with differently prepared HNF samples. The value for raw HNF was found to be 5 mL/g, which was then reduced to 3.2 mL/g when the raw HNF sample were purified [98].

Auto ignition test at a heating rate of 5°C/min was also performed to analyze the thermal stability of the compound. It was found that HNF ignited spontaneously at the temperature between 129°C–131°C. The results from VTS at  $60^{\circ}$ C/48 h were extrapolated and converted to  $80^{\circ}$ C and  $90^{\circ}$ C for 40 h. It was found that the value for the gas evolved at  $60^{\circ}$ C and  $80^{\circ}$ C were less than  $1.2 \, \text{mL/g} \, [118]$ .

It is observed that gas begins to evolve at temperatures higher than 60°C–80°C. It can be inferred that the rate of decomposition of HNF would be much lower at room temperature. Thermal instability is seen only in elevated temperatures, making HNF relatively stable at room temperature under normal storage conditions.

#### 2.3 | Thermal Characteristics

The thermal decomposition of HNF has been studied extensively, with a particular focus on the formation of intermediates and final products. It is reported that the primary decomposition products of HNF include HZN ( $N_2H_4$ ), ammonia ( $NH_3$ ), and nitrous oxide ( $N_2O$ ), with significant amounts of nitrogen dioxide ( $NO_2$ ) observed at higher temperatures. The decomposition begins in the solid phase with the formation of a foamy layer near the surface. As the material heats up, gas bubbles form within this layer, releasing gaseous species that subsequently ignite in the gas phase [68].

The thermal decomposition of HNF follows an endothermic reaction in the initial stages, which transitions to an exothermic process as the temperature increases. The simplified net decomposition pathway for HNF under thermal conditions can be summarized by the following reactions:

HNF (solid) 
$$\rightarrow$$
 N<sub>2</sub>H<sub>4</sub> + NO<sub>2</sub> ( $\Delta H = +45.6 \text{ kJ/mol}$ ) (6)

$$N_2H_4 + NO_2 \rightarrow N_2 + NO + 2H_2O (\Delta H = -241.8 \text{ kJ/mol})$$
 (7)

These reactions demonstrate the high-energy content of HNF and its potential for use in propulsion systems. The presence of exothermic reactions in the later stages of decomposition helps sustain the flame and contributes to the overall energy release during combustion [68].

#### 2.3.1 | Decomposition Kinetics and Mechanisms

Thermal analysis techniques, such as differential scanning calorimetry (DSC) and thermogravimetric analysis (TGA) coupled with DTA, have been instrumental in studying the thermal behavior of HNF. DTA measurements on HNF samples have revealed distinct exothermic peaks at temperatures around 109°C and 134°C-139°C, indicative of decomposition processes [112]. This observation aligns with findings from TGA experiments, where significant mass loss was observed above 105°C, suggesting rapid decomposition of HNF [98]. These results provide valuable information about the decomposition temperature range and kinetics of HNF, which is essential for its storage and handling in practical applications. Moreover, studies [68, 98, 112] have investigated the influence of heating rates on the thermal decomposition of HNF, revealing variations in decomposition behavior. For instance, DSC experiments conducted at different heating rates have shown that higher heating rates can lead to changes in the temperature profile of exothermic peaks, indicating ratedependent decomposition kinetics. Similarly, TGA experiments conducted with varying heating rates have provided insights into the kinetics of HNF decomposition, allowing for the determination of activation energy and reaction order parameters. These findings underscore the importance of considering heating rates in thermal analysis studies to accurately characterize the decomposition behavior of HNF.

Thermal analysis of HNF reveals a two-stage decomposition behavior, as evidenced by DSC and TGA [119]. The DSC curve, Figure 10, exhibited two distinct exothermic peaks, with max-

imum decomposition temperatures ( $T_{\rm max}$ ) observed at approximately 136°C and 138°C. The activation energy ( $E_{\rm a}$ ) for the first and second exotherms was determined using the Kissinger method, yielding a value of 150 kJ/mol (for both exotherms) with pre-exponential factors of  $1.3\times10^{19}$  and  $1.5\times10^{19}$ , respectively. These results were corroborated by the Ozawa method, which produced a similar activation energy of 149 kJ/mol.

TG studies further supported the two-stage decomposition process [119], as shown in Figure 11. The first stage, occurring within the temperature range of 105°C–142°C, accounted for a significant 72.5% weight loss, while the second stage, spanning 142°C–210°C, resulted in an additional 24.5% weight loss. This weight loss pattern suggests the formation of cyanamide-type species during the thermal decomposition of HNF, likely due to the rapid breakdown of HNF and recombination of its decomposition products. These observations are consistent with prior studies by Schoyer et al. [109] and Williams and Brill [68], who identified ANF as an intermediate during the slow decomposition of HNF, with ANF further decomposing into AN.

The thermal studies underline the critical role of cyanamide-type species and nitro and amino groups in the decomposition process, offering valuable insights for understanding the thermal stability and reaction kinetics of HNF. These findings not only align closely with previously reported data but also provide a reliable foundation for modeling HNF combustion and optimizing its application in green propellants.

In addition to thermal analysis techniques, studies have utilized infrared (IR) and Raman spectroscopy to investigate the decomposition mechanisms of HNF [120-122]. IR spectroscopy has been particularly useful in identifying the primary decomposition products of HNF and elucidating reaction pathways [123]. For example, IR spectra of HNF samples heated to different temperatures have shown characteristic absorption bands corresponding to the formation of NF, HZN, nitrogen oxides, and other decomposition products. Similarly, Raman spectroscopy has provided complementary information about the molecular structure and vibrational modes of HNF during decomposition, aiding in the identification of reaction intermediates and products. Together, these spectroscopic techniques offer valuable insights into the chemical transformations occurring during the thermal decomposition of HNF. Furthermore, studies have explored the effect of catalysts on the thermal decomposition of HNF, aiming to enhance reaction kinetics and product yields. For instance, catalytic decomposition experiments conducted with platinum/alumina-silica catalysts have shown changes in the decomposition pathways and product distributions compared to thermal decomposition alone [122]. Specifically, the presence of catalysts has been found to lower the decomposition temperature of HNF and promote the formation of specific decomposition products, such as nitrogen oxides and carbon monoxide. These results highlight the potential for catalytic processes to modulate the decomposition behavior of HNF and improve its utility in practical applications.

In addition to experimental studies, theoretical modeling approaches have been employed to explain the mechanisms of HNF decomposition at the molecular level [123]. Quantum chemical calculations using density functional theory (DFT), and

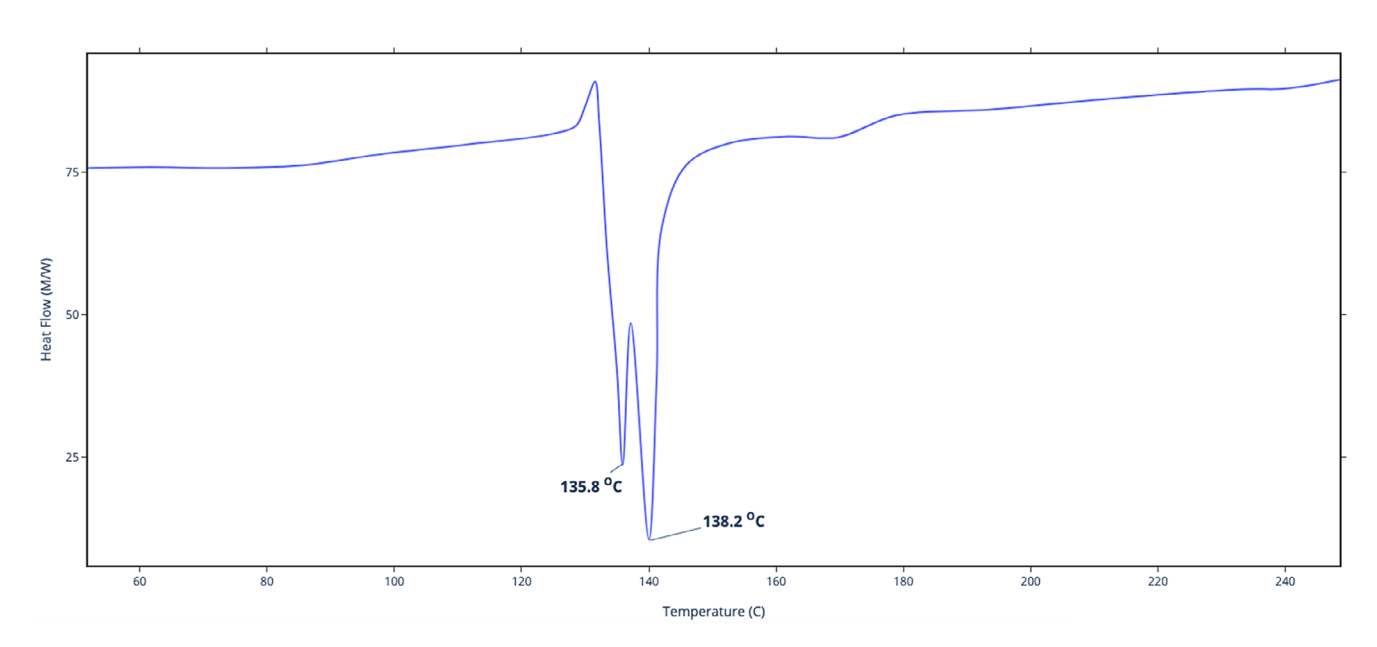


FIGURE 10 DSC analysis of HNF sample weight 4 mg, heating rate 10°C/min, and N<sub>2</sub> gas at 60 L/h. Adapted from [119].

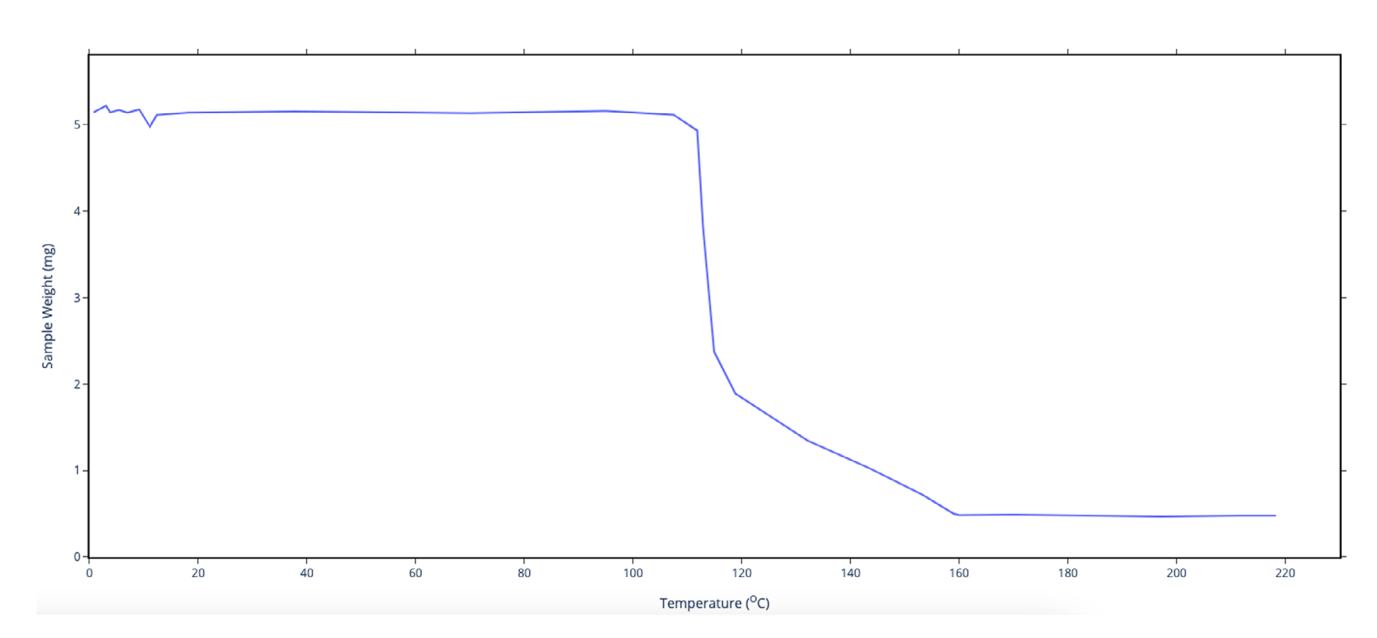


FIGURE 11 | TGA analysis of HNF sample weight 4.91 mg, heating rate 10°C/min. Adapted from [119].

ab initio methods have provided insights into the energetics and reaction pathways of HNF decomposition reactions [124]. For example, computational studies have predicted the formation of NF and HZN as primary decomposition products, which is consistent with experimental observations. Moreover, theoretical calculations have explained the role of solvent effects and reaction intermediates in influencing the decomposition kinetics and product distributions of HNF. These theoretical insights complement experimental findings and contribute to a comprehensive understanding of the decomposition mechanisms of HNF. The condensed phase decomposition of HNF is a multifaceted process crucial for understanding its combustion behavior [125]. Initiated by proton transfer and subsequent NF decomposition, this process leads to the formation of radicals like OH and NO2, which interact with HZN to produce various decomposition products, including ANF, nitrogen oxides, water, and carbon-containing compounds. The heat generated, estimated at 305.4 kJ/mol, plays a pivotal role in determining burning rates. Computational models based on condensed-phase chemistry facilitate the calculation of rate constants for leading combustion reactions, demonstrating alignment with experimental observations. The activation energy for HNF decomposition closely resembles autocatalytic values, suggesting a nuanced interplay of reactions with varying activation energies. This emphasizes the dominant influence of condensed-phase chemistry on HNF combustion, ensuring stability across a broad pressure spectrum. Further investigation into these mechanisms promises insights vital for optimizing propellant formulations and enhancing combustion efficiency.

Overall, the thermal decomposition of HNF is a complex process influenced by various factors, including temperature, heating rate, catalysts, and molecular structure. Experimental techniques such as DSC, TGA, IR spectroscopy, and Raman spectroscopy have provided valuable insights into the thermal behavior and decomposition mechanisms of HNF, while theoretical modeling approaches have offered a molecular-level understanding of the underlying processes. Continued research efforts in this field are essential to further understand the decomposition kinetics and mechanisms of HNF, enabling its optimization for various applications in propulsion and energetics.

#### 2.3.2 | Combustion Behavior and Mechanism

The combustion behavior of HNF has been extensively studied, focusing on surface burning, flame structure, pressure exponent, and BRM effects. Understanding these aspects is crucial for optimizing HNF-based propellants for various applications, including rocket propulsion. In this section, we explore the findings of key studies, explaining the intricate details of HNF combustion. HNF combustion exhibits a distinct two-zone flame structure, as revealed by various experimental techniques. Thin thermocouples placed at different distances from the burning surface have provided insights into temperature profiles during combustion. Laser Doppler anemometry (LDA) studies have further elucidated the flame structure, identifying three regions: the fizz zone, dark zone, and luminous flame zone. Investigations using LDA and coherent anti-Stokes Raman spectroscopy (CARS) have shed light on velocity and temperature profiles above the burning surface, highlighting the presence of aerosols and gaseous reactants in the primary reaction zone and nonluminous zone [126, 127].

The burning rate of HNF can be affected by several factors, including pressure and the presence of BRMs. Under standard conditions, HNF shows a high-pressure exponent, indicating a strong dependence of the burning rate on pressure. For example, HNF exhibits a pressure exponent *n* of approximately 0.85, which is higher than the value of 0.6, a target value for propellant applications. Studies using temperature-jump/Fourier transform infrared (FTIR) spectroscopy revealed that the decomposition of HNF occurs in three distinct stages [98, 112]. In the first stage (below 123°C), only preheating is observed. The second stage (123°C-260°C) involves the formation of ANF, which subsequently breaks down into AN and other decomposition products like N<sub>2</sub>O, H<sub>2</sub>O, and CO. At temperatures above 260°C, deflagration is observed, resulting in the formation of CO<sub>2</sub> and other gaseous products. The presence of catalysts such as platinum further modifies the decomposition process, increasing the amounts of CO2 produced and altering the nature of the products captured in cold traps.

### 2.3.3 | Surface Burning and Flame Structure of HNF

The surface burning characteristics and flame structure of HNF have been studied extensively using advanced diagnostic techniques [128]. The flame structure of HNF is observed to have a two-zone configuration with a distinct dark zone between the fizz zone and the luminous flame zone [68, 129]. The flame temperature profile, as measured by tungsten-rhenium

thermocouples, shows that at low pressure, the temperature in the first zone is between 1320 and 1540 K, while the second zone ranges from 2300 and 2720 K [129]. The flame structure of HNF combustion provides insights into the reaction mechanisms and energy release processes. Understanding the flame zones is essential for modeling and optimizing propellant performance.

**2.3.3.1** | **Three-Zone Flame Structure.** Experimental studies have revealed that HNF combustion typically exhibits a three-zone flame structure: the fizz zone, dark zone, and luminous flame zone.

Fizz zone: Located closest to the burning surface, this zone is characterized by turbulent gas release and rapid temperature and pressure rises. Here, the decomposition of HNF molecules releases species such as nitrogen  $(N_2)$ , water vapor  $(H_2O)$ , nitrogen dioxide  $(NO_2)$ , and other intermediates. LDA studies showed high gas velocities and significant heat transfer in this region, indicating intense surface reactions [129].

*Dark zone*: Situated between the fizz zone and the luminous flame zone, the dark zone exhibits lower light emission, suggesting incomplete combustion or the presence of intermediate reaction stages. This zone is associated with a slower rate of gas-phase reactions and continued heat transfer to the propellant surface. It was observed that the dark zone plays a crucial role in sustaining the combustion wave by maintaining thermal energy transfer [126, 127].

*Luminous flame zone*: The outermost region of the flame is where complete combustion occurs, leading to the formation of final products such as nitrogen  $(N_2)$ , water vapor  $(H_2O)$ , and carbon dioxide  $(CO_2)$ . CARS studies confirmed the presence of these stable end-products, which contribute to the visible luminosity of the flame [126, 127, 129]

These flame characteristics are unique to HNF when compared to other oxidizers, such as AP, which exhibits a less distinct dark zone. This difference suggests that the thermal decomposition of HNF proceeds through intermediate stages that strongly affect its burning behavior.

#### 2.3.4 | Pressure Exponent and BRM Effects

One of the most critical parameters in solid propellant combustion is the pressure exponent (n), which dictates how the burning rate (r) changes with pressure (p), has been a focus of investigation to optimize HNF-based propellants. This relationship is typically expressed through Vieille's law (8):

$$r = a \times p^n \tag{8}$$

where a is a proportionality constant. For practical applications in rocketry, the value of n should ideally be less than 0.6 to ensure stable combustion.

For HNF, the pressure exponent has been reported to vary significantly depending on the formulation and the presence of BRMs. Some researchers reported a pressure exponent of 0.85 and higher for neat HNF. This high-pressure exponent can lead to unstable

combustion and poses challenges for controlling the burning rate in rocket motors. To address this issue, researchers have explored the use of BRMs to reduce the pressure exponent and enhance combustion stability. Studies have explored the use of BRMs to modify the pressure exponent and enhance combustion efficiency. Selective catalytic reduction (SCR) catalysts, such as  $V_2O_5$ , have shown promising results in increasing the burning rate of HNF. However, achieving the desired pressure exponent of 0.5 remains a challenge due to compatibility issues with HNF. Researchers working in the field have identified potential BRMs compatible with HNF, leading to significant reductions in the pressure exponent [124].

### 2.4 | Propellant Composition

AP-based solid propellant grains have been the workhorse for the space launch industry for decades. Even with all the negative traits of AP, space agencies of all the world's leading countries in the rocket launch business use HTPB/AP-based solid rocket motors for their space missions [130-133]. Many compositions have been tried and tested against the conventional HTPB/APbased compositions for various ballistic and performance characteristics. Fine-tuning of propellant formulations, either through the introduction of alternative oxidizers like AP or through the application of specific catalysts, has shown promise in achieving the desired pressure exponent while meeting other performance criteria. The ballistic properties of HNF-based propellants can be modified by varying the particle size of the oxidizer. Fine HNF particles, obtained through grinding processes, have been investigated for their impact on propellant burning rates. Studies have shown that the use of fine HNF particles leads to a reduction in the pressure exponent, indicating improved combustion characteristics. In addition, the combination of fine and coarse HNF particles offers a means to tailor propellant properties to specific requirements. The combustion mechanism of propellants containing fine HNF particles closely resembles the sequential burning of oxidizer particles and the binder, contributing to enhanced combustion efficiency [134].

# 2.4.1 | Performance Comparison With Conventional Compositions

Most often the comparison of HNF is made with AP as there is a strict need to find an eco-friendly green alternative as discussed in the previous sections. The replacement of AP by HNF would also result in the replacement of HTPB, the most used polymeric binder. This would require additional additives to the composition, which would eventually reduce the loading ratio of fuel high-energy fuel and oxidizer.

NASA Lewis code was used to obtain a theoretical value of specific impulse for the two propellant combinations, that is, Al/AP/HTPB and Al/HNF/GAP, for application in defense and space sectors. For space application, the calculated specific impulse for HNF composition was found to be approximately 7% more than that of the AP composition. Similarly, for the defense applications, the combination of AP/HTPB and HNF/GAP with 4% Al as additives were theoretically compared, resulting in the composition of HNF outperforming the AP composition by

approximately 12% when compared to their specific impulse [72, 135]. It can be seen from the experiments conducted by Schoöyer et al. that the CSP grain composition consisting of HNF with Al and GAP/BAMO outperformed the AN-based composition as well [136].

Performance comparison between AP and HNF can be seen in an actual scenario through the experiment on the booster of Ariane 5 (HERMES launch) conducted by Schoever et al. Table 5 presents a comparative analysis of various conventional solid propellant compositions along with a composition consisting of HNF as an oxidizer with different binders. It was found that when replacing the oxidizer in the composition of AL/AP/HTPB with HNF, the specific impulse got an increment of 7% along with an increase of 10% in the payload capacity. A similar trend was observed when the oxidizer in SEP Moteur d'Apogee Geostationaire European (MAGE) was replaced by HNF, which resulted in a 5%-6% decrease in the propellant mass required for 700-1200 kg satellite. Rise in the specific impulse from 2825-2884 to 3021-3090 m/s was also observed when replacing the combination of AP and carboxyl-terminated polybutadiene (CTPB) by HNF and GAP combination [112].

Calculation shows that with chamber pressure of 10 MPa and nozzle exit to throat area ratio of 100, the specific impulse in equilibrium flow of 59% HNF/21% Al/20% GAP propellant was 215.5 N-s/kg higher than that of 76% AP/13% A1/11% HTPB propellant [138]. A similar comparison between these two oxidizers was conducted with BNDPAF (bis-(2,2-dinitropropyl) acetal/formal mixture) as an additive to Al/GAP-based formulation. It was seen that the HNF-based composition gave a specific impulse of 2703.82 N s/kg whereas for the composition with AP, the value for specific impulse was 2594.06 N s/kg [93].

It has been reported that the various combustion parameters, such as the combustor temperature, characteristic velocity, and so forth, showed an increment when parts of oxidizer in AP-based composition were replaced by HNF. This shows a positive energy performance of the solid propellant. Though low on the OB when compared to standalone AP, this provided some added advantages for the defense application. Due to less oxygen, the amount of  $Al_2O_3$ ,  $CO_2$ , and  $H_2O$  is reduced, reducing the exhaust gas plume radiation characteristics. This results in less detectable missiles and launch sites [139]. Propellant combinations of HNF, GAP/BAMO with 35% diborane or 29% pentaborane are also under consideration as an alternative to the conventional composition [136].

## 2.4.2 | BRMs

Various techniques have been tested to alter the burn rate of HNF-based compositions. In one of the studies, a portion of HNF was replaced with AP and Al, which drastically increased the pressure coefficient value to 1.2. Later, when the composition was tested with GAP as the binder, the pressure coefficient ranged between 0.65 and 0.88 [140]. Tummers et al. tested unsupported  $V_2O_5$  and alumina support  $Mn_3O_4$  as BRMs for pressed HNF pellets. The inclusion of these catalysts resulted in an 11-fold increase in the burning rate along with the pressure coefficient reducing to 0.28 [141, 142].

**TABLE 5** | Specific impulse comparison of different solid propellant compositions.

		Fuel				Max Isp <sub>vac</sub>	Flame	Ref.
Oxidizer	wt%	Binder	wt%	Additive	wt%	(m/s)	temp (K)	
Composition	with only e	nergetic binde	r					
	80	HTPB	20	No metallic/non-	_	2713.0	2266	[117, 135]
AP				metallic additives				
	78	GAP	22	included		3053.0	_	
	77	PLN	23			3052.0	_	
	64	PGN	36			3054.0	_	
	80	HTPB	20			2412.0	1420	
AN		~						
	80	GAP	20			2711.0	2353	
	80	PLN	20			2731.0	_	
	75	PGN	25			2816.0	_	
HNF	80	HTPB	20			2853.0	_	
11111	80	GAP	20			3218.0	3275	
	80	PLN	20			3227.0	3321	
	80	PGN	20			3282.0	3318	
	80	BAMO	20			3381.0	3381	[117]
	80	GAP	20			3150.0	3132	[]
ADN								
	80	PGN	20			2938.0	2900	
	80	PLN	20			3111.0	3018	
	80	BAMO	20			3175.0	3139	
Composition	with metall	ic/non-metall	ic fuel and	energetic binder				
	76	HTPB	11	Al	13	3202.0	_	[135]
AP								
	60	HTPB	20		20	3086.0		
	54	GAP	23		23	3297.0		
	57	GAP	20		23	3027.4		[136, 137]
	32	PGN	44		24	3278.0		[135]
	49	PLN	27		24	3295.0		
	53	HTPB	20		27	3084.0		
AN								
	52	GAP	20		28	3279.0		
	37	PGN	34		29	3279.0		
	50	PLN	20		30	3291.0		
HNF	61	HTPB	20		19	3211.0		
11141.	59	GAP	20		21	3436.0		
	60	PGN	20		20	3438.0		
	60				20			
	70	PLN GAP	20 20	$\mathrm{B}^{\mathrm{a}}$	10	3434.0 3042.3		[136, 137]
A D				D				[130, 137]
AP Boron.	68	GAP	20		12	2911.0		

<sup>&</sup>lt;sup>a</sup>Boron.

#### 2.4.3 | Compatibility With Binders

Conventionally used binders such as HTPB and CTPB have unsaturated double bonds present in their chemical structure. HNF tends to attack the double bond present in these compounds and produces gas as the reaction product [137]. The released gas swells the propellant grain, making it porous, which further softens and weakens the grain. There is a loss of structural strength and degradation of mechanical properties due to attacks on the double bonds. The propellant grain prepared using saturated binders, that is, without any double bonds, does not show any such degradation but has low performance compared to the AP/HTPB combination [135, 143, 144]. A similar deteriorating phenomenon can be observed in compositions containing curing agents such as tris(1-(2-methyl)aziridinyl)phosphine oxide (MAPO) and curing agents of GAP and HTPB-containing isocyanates, where binder and HNF tend to compete for reacting with isocyanates. The mixtures of HNF with GAP and HNF with isocyanates in 1:1 ratio were tested under the VTS test. It was found that the gas that evolved during these two tests was way above the acceptable limit. Particularly for HNF + isocyanate composition, the value was above 100 mL gas evolved per gram of the composition at even 23 h of testing [112, 143, 145].

#### 2.4.4 | Bonding Agent and Mechanical Strength

Due to a lack of knowledge of bonding agents for HNF, the cured grain, consisting of HNF, would lack mechanical strength compared to that of the AP. Thus, it was found that any Lewis acid can be used as the bonding agent in the composition. The Lewis acid can be anything, such as boron or boron-containing compounds, antimony pentachloride, titanium halides, zirconium tetrachloride, and so forth. As per the invention, these bonding agents would coat the surface of HNF particles and, with the addition of polymeric binder, would react to form an adhesive or chemical bond, providing the required structural strength. Dichloromethane was used to coat the surface of the HNF particle, thus preventing direct contact with the binder [146].

Studies conducted lately propose the use of newly discovered energetic binders such as GAP, poly-nitromethyl oxetane (PLN) and poly-glycidyl nitrate (PGN) instead of conventional ones. It was reported that the use of GAP, PLN, and PGN tends to show improvement in the combustion properties when compared to that of AP/HTBP combination [68, 135]. Additives such as nitroguanidine and triethylene melamine can be incorporated into the composition containing unsaturated compounds to overcome compatibility issues. The addition of a minimum 2 wt% of nitroguanidine during the mixing phase while using the unsaturated binders can also increase the shelf life significantly [145].

The use of poly-isocyanate curing agents eliminates the incompatibility between HNF and HTPB. Poly-isocyanates such as polymethylene polyphenyl isocyanate (PAPI), toluene di-isocyanate (TDI) and hexamethylene di-isocyanate (HMDI) can be used as curing agents for HTPB containing propellant grain. PAPI is preferred over the others owing to better shelf life at the

lowest ratio for isocyanate and hydroxyl groups(NCO/OH ratio), resulting in the least urethane linkage formation, as compared to the other candidates [143, 144].

# 2.5 | Critical Evaluation of Existing HNF Studies and Discussion

A comparative analysis of HNF studies reveals both advancements and limitations in the current understanding of HNF combustion. Studies utilizing laser diagnostics, such as LDA and CARS, have provided detailed insights into the flame structure and temperature profiles of HNF [129]. These techniques have been instrumental in identifying the distinct zones within the flame and understanding the impact of pressure on the combustion behavior.

However, discrepancies exist between different studies regarding the pressure exponent and the effectiveness of BRMs. For instance, while some studies report a pressure exponent reduction to 0.28 with V<sub>2</sub>O<sub>5</sub> catalysts [142], others indicate challenges with catalyst compatibility and varying performance across different pressure ranges [68, 123, 125, 129, 141]. This inconsistency highlights the need for further research to address the limitations of current BRMs and improve their compatibility with HNF. In addition, the thermal decomposition studies provide valuable data on the activation energy and intermediate species involved in HNF combustion [68, 112, 120, 121]. However, the complexity of the decomposition process and the presence of multiple intermediate species make it challenging to develop accurate computational models. The dispersed state of aerosols and gaseous reactants in near-surface regions adds further complexity to modeling efforts.

The critical evaluation of existing HNF studies emphasizes the need for continued research to address the identified gaps. Future research directions should focus on the following areas:

Improved understanding of combustion mechanisms: Enhanced diagnostic techniques and modeling approaches are required to gain a deeper understanding of the combustion mechanisms of HNF. This includes studying the interactions between different flame zones and the impact of intermediate species on overall combustion behavior.

Optimization of BRMs: Research should focus on developing and testing new BRMs that are both effective and compatible with HNF. High-temperature catalysts and coating particles offer potential solutions, but their performance and compatibility need further investigation.

Researching for new polymeric binders: The incompatibility of the present polymer binder with HNF can be addressed by the inclusion of various secondary agents. However, these agents can take up some portion of the binder composition. Therefore, it is essential to develop alternative binders to advance the usage of HNF in solid rocket motors.

Advanced computational modeling: The development of more accurate computational models is essential for predicting the combustion behavior of HNF. This includes incorporating the

complex interactions between different flame zones, aerosols, and gaseous reactants.

*Pressure-dependent behavior*: Further studies are needed to understand the pressure-dependent behavior of HNF and its impact on combustion characteristics. This includes investigating the effects of pressure on flame structure, temperature profiles, and overall performance.

#### 3 | Conclusion

HNF holds significant promise as a next-generation green oxidizer due to its high energy output, reduced environmental impact, and favorable combustion characteristics. Despite its low impact and friction sensitivity values, which are already within safe handling limits, these properties can be further optimized to enhance their application in propulsion systems. The needle-like crystal morphology of HNF presents challenges in achieving high solid loading within propellant formulations, which may limit its OB compared to AP. However, its positive heat of formation and higher heat of explosion make it an excellent candidate for energy-dense propellants.

The inclusion of HNF in AP-based formulations has been shown to improve combustion parameters such as chamber temperature and characteristic velocity, demonstrating its superior energy performance. While HNF has a lower OB, this results in reduced emissions of  ${\rm Al_2O_3}$ ,  ${\rm CO_2}$ , and  ${\rm H_2O}$ , which significantly decreases the exhaust plume's radiation characteristics. This property makes HNF-based propellants particularly advantageous for defense applications, enabling less detectable missile launches and reduced visibility of launch sites.

From a combustion perspective, this review has provided a comprehensive analysis of HNF's flame structure, combustion mechanisms, and behavior under different conditions. The threezone flame structure—comprising the fizz zone, dark zone, and luminous flame zone—highlights the complexity of HNF combustion. Critical insights into the pressure-dependent characteristics of HNF reveal its high-pressure exponent, which can be addressed through the use of BRMs. Catalytic agents like  $\rm V_2O_5$  have shown a potential to significantly enhance the burn rate while reducing the pressure exponent, but further research is needed to overcome compatibility challenges.

In terms of thermal decomposition, HNF exhibits a two-stage process that produces intermediate compounds like ANF. These intermediates decompose further into AN and gaseous products such as  $N_2O$ ,  $H_2O$ , and CO. The formation of cyanamide-type species during decomposition has been observed, which underscores the need for precise control over synthesis and handling. Advances in synthesis methodologies, such as ultrasonic vibration and cryogenic crystallization, have improved HNF's purity and stability, offering pathways for safer and more efficient production.

This review also highlights the *limitations* of HNF. Its needle-like morphology reduces solid loading in compositions and increases the required stoichiometry compared to AP. In addition, HNF-based formulations face challenges in achieving compatibility

with conventional binders like HTPB and its curing agents that contain isocyanates as functional groups due to its reactivity with double bonds. While the use of alternative binders like GAP and additives like nitroguanidine has shown promise, further optimization is needed to ensure mechanical strength and stability.

Overall, this study contributes to a deeper understanding of HNF combustion, paving the way for its application in environmentally friendly propulsion systems. By combining its inherent advantages with advancements in formulation and diagnostic technologies, HNF can play a pivotal role in the development of high-performance green propellants for both space and defense applications.

#### **Data Availability Statement**

Data sharing not applicable to this article as no datasets were generated or analysed during the current study.

#### References

- 1. G. P. Sutton and O. Biblarz, "Chapter 1, Classification Rocket Propulsion Elements," in *Rocket Propulsion Elements* (John Wiley & Sons, 2011), 4–24.
- 2. J. D. Anderson Jr. "Introduction to Flight," in *The Art of Flight*, 7th ed. (American Institute of Aeronautics and Astronautics, 2016), 1–14, https://doi.org/10.2514/5.9781624103735.0001.0014.
- 3. K. Schmidt-Rohr, "Why Combustions Are Always Exothermic," *Journal of Chemical Education* 92 (2015): 2094–2099, https://doi.org/10.1021/acs.jchemed.5b00333.
- 4. M. W. Beckstead, R. L. Derr, and C. F. Price, "A Model of Composite Solid-Propellant Combustion Based on Multiple Flames," *AIAA Journal* 8 (1970): 2200–2207, https://doi.org/10.2514/3.6087.
- 5. N. Kubota, *Propellants and Explosives: Thermochemical Aspects of Combustion*, 2nd ed. (Wiley, 2007), https://doi.org/10.1002/9783527610105.
- 6. C. T. Brandon, F. S. Steven, and E. G. Ibrahim, "Solid-Rocket Propellants," US10519075B2 (2019).
- 7. M. Tremblay, G. Perrault, and G. Duchesne, "Solid Propellants Containing Polyether or Polyester Binders," US4156700A (1979).
- 8. M. Q. Brewster, T. A. Sheridan, and A. Ishiharat, "Ammonium Nitrate-Magnesium Propellant Combustion and Heat Transfer Mechanisms," *Journal of Propulsion and Power* 8 (1992): 760–769, https://doi.org/10.2514/3.23547.
- 9. A. C. Foltran, D. F. Moro, N. D. Pereira da Silva, A. E. G. Ferreira, L. K. Araki, and C. H. Marchi, "Burning Rate Measurement of KNSu Propellant Obtained by Mechanical Press," *Journal of Aerospace Technology and Management* 7 (2015): 193–199, https://doi.org/10.5028/jatm.v7i2.431.
- 10. M. K. Bharti, L. Bansal, and S. Chalia, "Catalytic Potential of Microsized Additives In Enhancing The Linear Burn Rate of Potassium Nitrate-Sucrose Based Composite Solid Propellant Strands," *International Journal of Energetic Materials and Chemical Propulsion* 20 (2021): 61–77, https://doi.org/10.1615/IntJEnergeticMaterialsChemProp.2021038209.
- 11. S. K. Pradhan, V. Kedia, and P. Kour, "Review on Different Materials and Their Characterization as Rocket Propellant," *Materials Today: Proceedings* 33 (2020): 5269–5272, https://doi.org/10.1016/j.matpr.2020.02.960.
- 12. S. Elbasuney, A. Fahd, and H. E. Mostafa, "Combustion Characteristics of Extruded Double Base Propellant Based on Ammonium Perchlorate/Aluminum Binary Mixture," *Fuel* 208 (2017): 296–304, https://doi.org/10.1016/j.fuel.2017.07.020.

- 13. C. Griego, N. Yilmaz, and A. Atmanli, "Analysis of Aluminum Particle Combustion in a Downward Burning Solid Rocket Propellant," *Fuel* 237 (2019): 405–412, https://doi.org/10.1016/j.fuel.2018.10.016.
- 14. L. Liu, F. Li, L. Tan, L. Ming, and Y. Yi, "Effects of Nanometer Ni, Cu, Al and NiCu Powders on the Thermal Decomposition of Ammonium Perchlorate," *Propellants, Explosives, Pyrotechnics* 29 (2004): 34–38, https://doi.org/10.1002/prep.200400026.
- 15. T. Miller and J. Herr, "Green Rocket Propulsion by Reaction of Al and Mg Powders and Water," paper presented at 40th AIAA/ASME/SAE/ASEE Joint Propulsion Conference and Exhibit, Fort Lauderdale, FL, July 11–14, 2004, https://doi.org/10.2514/6.2004-4037.
- 16. Z. Liu, S. Li, M. Liu, D. Guan, X. Sui, and N. Wang, "Experimental Investigation of the Combustion Products in an Aluminised Solid Propellant," *Acta Astronautica* 133 (2017): 136–144, https://doi.org/10.1016/j.actaastro.2017.01.025.
- 17. R. Lade, K. Wasewar, R. Sangtyani, A. Kumar, D. Shende, and D. Peshwe, "Influence of the Addition of Aluminium Nanoparticles on Thermo-Rheological Properties of Hydroxyl-Terminated Polybutadiene-Based Composite Propellant and Empirical Modelling," *Journal of Thermal Analysis and Calorimetry* 138 (2019): 211–223, https://doi.org/10.1007/s10973-019-08149-0.
- 18. H. Belal, C. W. Han, I. E. Gunduz, V. Ortalan, and S. F. Son, "Ignition and Combustion Behavior of Mechanically Activated Al–Mg Particles in Composite Solid Propellants," *Combustion and Flame* 194 (2018): 410–418, https://doi.org/10.1016/j.combustflame.2018.04.010.
- 19. M. Abd-Elghany, A. Elbeih, T. M. Klapötke, and M. Abdelhafiz, "Performance of Advanced Composite Solid Rocket Propellants Based on Novel Oxidizers," *IOP Conference Series: Materials Science and Engineering* 610 (2019): 012002, https://doi.org/10.1088/1757-899X/610/1/012002
- 20. M. B. Talawar, R. Sivabalan, T. Mukundan, et al., "Environmentally Compatible Next Generation Green Energetic Materials (GEMs)," *Journal of Hazardous Materials* 161 (2009): 589–607, https://doi.org/10.1016/j.jhazmat.2008.04.011.
- 21. R. M. Richard and D. W. Ball, "B3LYP Calculations on the Thermodynamic Properties of a Series of Nitroxycubanes Having the Formula  $C_8H_{8-x}(NO_3)_x$  (x=1–8)," *Journal of Hazardous Materials* 164 (2009): 1595–1600, https://doi.org/10.1016/j.jhazmat.2008.09.078.
- 22. S. Chaturvedi and P. N. Dave, "Solid Propellants: AP/HTPB Composite Propellants," *Arabian Journal of Chemistry* 12 (2019): 2061–2068, https://doi.org/10.1016/j.arabjc.2014.12.033.
- 23. G. Steinhauser and T. M. Klapötke, ""Green" Pyrotechnics: A Chemists' Challenge," *Angewandte Chemie International Edition* 47 (2008): 3330–3347, https://doi.org/10.1002/anie.200704510.
- 24. M. Ravanbod and H. R. Pouretedal, "Catalytic Effect of  $Fe_2O_3$ ,  $Mn_2O_3$ , and  $TiO_2$  Nanoparticles on Thermal Decomposition of Potassium Nitrate," *Journal of Thermal Analysis and Calorimetry* 124 (2016): 1091–1098, https://doi.org/10.1007/s10973-015-5167-y.
- 25. R. Turcotte, R. C. Fouchard, A. M. Turcotte, and D. E. G. Jones, "Thermal Analysis of Black Powder," *Journal of Thermal Analysis and Calorimetry* 73 (2003): 105–118, https://doi.org/10.1023/A:1025181424038.
- 26. R. G. Reddy, T. Wang, and D. Mantha, "Thermodynamic Properties of Potassium Nitrate–Magnesium Nitrate Compound [2KNO<sub>3</sub>·Mg(NO<sub>3</sub>)<sub>2</sub>]," *Thermochimica Acta* 531 (2012): 6–11, https://doi.org/10.1016/j.tca.2011.12.010.
- 27. Q. Jia, P. Deng, X. Li, L. Hu, and X. Cao, "Insight Into the Thermal Decomposition Properties of Potassium Perchlorate (KClO<sub>4</sub>)-Based Molecular Perovskite," *Vacuum* 175 (2020): 109257, https://doi.org/10.1016/j.vacuum.2020.109257.
- 28. C. Wu, K. Sullivan, S. Chowdhury, G. Jian, L. Zhou, and M. R. Zachariah, "Encapsulation of Perchlorate Salts Within Metal Oxides for Application as Nanoenergetic Oxidizers," *Advanced Functional Materials* 22 (2012): 78–85, https://doi.org/10.1002/adfm.201100479.

- 29. G. S. Tussiwand, V. E. Saouma, R. Terzenbach, and L. T. De Luca, "Fracture Mechanics of Composite Solid Rocket Propellant Grains: Material Testing," *Journal of Propulsion and Power* 25 (2009): 60–73, https://doi.org/10.2514/1.34227.
- 30. Z. Han, S. Sachdeva, M. I. Papadaki, and M. S. Mannan, "Ammonium Nitrate Thermal Decomposition With Additives," *Journal of Loss Prevention in the Process Industries* 35 (2015): 307–315, https://doi.org/10.1016/j.jlp.2014.10.011.
- 31. R. Gunawan and D. Zhang, "Thermal Stability and Kinetics of Decomposition of Ammonium Nitrate in the Presence of Pyrite," *Journal of Hazardous Materials* 165 (2009): 751–758, https://doi.org/10.1016/j.jhazmat.2008.10.054.
- 32. C. Oommen, "Ammonium Nitrate: A Promising Rocket Propellant Oxidizer," *Journal of Hazardous Materials* 67 (1999): 253–281, https://doi.org/10.1016/S0304-3894(99)00039-4.
- 33. L. Bansal, P. Jindal, and M. K. Bharti, "Investigations on the Modifications in Ignition Delay Time of Shellac-Based Pyrotechnic Igniter Using Additives of Varying Particle Size," *Journal of Aerospace Technology and Management* 12 (2020), e3820, https://doi.org/10.5028/jatm.v12.1178.
- 34. S. Elbasuney and M. Yehia, "Thermal Decomposition of Ammonium Perchlorate Catalyzed With CuO Nanoparticles," *Defence Technology* 15 (2019): 868–874, https://doi.org/10.1016/j.dt.2019.03.004.
- 35. S. Chaturvedi and P. N. Dave, "Nano-Metal Oxide: Potential Catalyst on Thermal Decomposition of Ammonium Perchlorate," *Journal of Experimental Nanoscience* 7 (2012): 205–231, https://doi.org/10.1080/17458080.2010.517571.
- 36. E. D. Petersen, F. A. Rodriguez, C. A. M. Dillier, J. C. Thomas, and E. L. Petersen, "Combustion Behavior of Ammonium Perchlorate at High Pressures," *AIAA Propulsion and Energy Forum and Exposition* (2019): 1–13, https://doi.org/10.2514/6.2019-4366.
- 37. V. V. Boldyrev, "Thermal Decomposition of Ammonium Perchlorate," *Thermochimica Acta* 443 (2006): 1–36, https://doi.org/10.1016/j.tca.2005. 11.038.
- 38. S. Chaturvedi and P. N. Dave, "A Review on the Use of Nanometals as Catalysts for the Thermal Decomposition of Ammonium Perchlorate," *Journal of Saudi Chemical Society* 17 (2013): 135–149, https://doi.org/10.1016/j.jscs.2011.05.009.
- 39. J. A. Conkling and C. J. Mocella, "Light and Color Production," in *Chemistry of Pyrotechnics*, C. Mocella and J. A. Conkling (CRC Press, 2019), 225–256, https://doi.org/10.1201/9780429262135-10.
- 40. W. H. Johnson and A. A. Gilliland, "Heat of Decomposition of Potassium Perchlorate," *Journal of Research of the National Bureau of Standards—Section A: Physics and Chemistry* (1961): 63, https://doi.org/10.6028/jres.065A.005.
- 41. V. M. H. Reyes, O. Martínez, and G. F Hernández, "National Center for Biotechnology Information." (Plant Breeding Universidad Autónoma Agraria Antonio Narro, 1923).
- 42. P. Kumar, "Advances in Phase Stabilization Techniques of AN Using KDN and Other Chemical Compounds for Preparing Green Oxidizers," *Defence Technology* 15 (2019): 949–957, https://doi.org/10.1016/j.dt.2019.03.002.
- 43. B. Zalba, J. M. Marıń, L. F. Cabeza, and H. Mehling, "Review on Thermal Energy Storage With Phase Change: Materials, Heat Transfer Analysis and Applications," *Applied Thermal Engineering* 23 (2003): 251–283, https://doi.org/10.1016/S1359-4311(02)00192-8.
- 44. M. K. Bharti and S. Chalia, "Depletion of Stratospheric Ozone by Chlorinated Exhaust of Ammonium Perchlorate Based Composite Solid Propellant Formulations: A Review," *International Journal of Research in Advanced Engineering and Technology* 3 (2017): 1–5.
- 45. M. S. Javadi, R. Søndergaard, O. J. Nielsen, M. D. Hurley, and T. J. Wallington, "Atmospheric Chemistry of *trans*-CF3CH=CHF: Products and Mechanisms of Hydroxyl Radical and Chlorine Atom Initiated

- Oxidation," Atmospheric Chemistry and Physics 8 (2008): 3141–3147, https://doi.org/10.5194/acp-8-3141-2008.
- 46. J. A. Dallas, S. Raval, J. P. Alvarez Gaitan, S. Saydam, and A. G. Dempster, "The Environmental Impact of Emissions From Space Launches: A Comprehensive Review," *Journal of Cleaner Production* 255 (2020): 120209, https://doi.org/10.1016/j.jclepro.2020.120209.
- 47. C. M. Steinmaus, "Perchlorate in Water Supplies: Sources, Exposures, and Health Effects," *Current Environmental Health Reports* 3 (2016): 136–143, https://doi.org/10.1007/s40572-016-0087-y.
- 48. M. R. Sijimol and M. Mohan, "Environmental Impacts of Perchlorate With Special Reference to Fireworks—A Review," *Environmental Monitoring and Assessment* 186 (2014): 7203–7210, https://doi.org/10.1007/s10661-014-3921-4.
- 49. J. Jos and S. Mathew, "Ammonium Nitrate as an Eco-Friendly Oxidizer for Composite Solid Propellants: Promises and Challenges," *Critical Reviews in Solid State and Materials Sciences* 42 (2017): 470–498, https://doi.org/10.1080/10408436.2016.1244642.
- 50. A. Deimling, W. Engel, and N. Eisenreich, "Phase Transitions of Ammonium Nitrate Doped With Alkali Nitrates Studied With Fast X-Ray Diffraction," *Journal of Thermal Analysis* 38 (1992): 843–853, https://doi.org/10.1007/BF01979416.
- 51. A. O. R. Sudhakar and S. Mathew, "Thermal Behaviour of CuO Doped Phase-Stabilised Ammonium Nitrate," *Thermochimica Acta* 451 (2006): 5–9, https://doi.org/10.1016/j.tca.2006.08.013.
- 52. P. Kumar, "An Overview on Properties, Thermal Decomposition, and Combustion Behavior of ADN and ADN Based Solid Propellants," *Defence Technology* 14 (2018): 661–673, https://doi.org/10.1016/j.dt.2018.03.009.
- 53. G. Da Silva, S. C. Rufino, and K. Iha, "An Overview of the Technological Progress in Propellants Using Hydroxyl-Terminated Polybutadiene as Binder During 2002–2012," *Journal of Aerospace Technology and Management* 5 (2013): 267–278, https://doi.org/10.5028/jatm.v5i3.242.
- 54. S. G. Il'Yasov, G. V. Sakovich, and A. A. Lobanova, "Synthesis, Structure, and Properties of *N,N'*-Dinitrourea," *Propellants, Explosives, Pyrotechnics* 38 (2013): 327–334, https://doi.org/10.1002/prep.20120 0030
- 55. Y. Wu, Y. Luo, and Z. Ge, "Properties and Application of a Novel Type of Glycidyl Azide Polymer (GAP)-Modified Nitrocellulose Powders," *Propellants, Explosives, Pyrotechnics* 40 (2015): 67–73, https://doi.org/10.1002/prep.201400005.
- 56. J. F. Pei, F. Q. Zhao, H. L. Lu, et al., "Compatibility Study of BAMO–GAP Copolymer With Some Energetic Materials," *Journal of Thermal Analysis and Calorimetry* 124 (2016): 1301–1307, https://doi.org/10.1007/s10973-016-5302-4.
- 57. P. Yin, J. Zhang, C. He, D. A. Parrish, and J. M. Shreeve, "Polynitro-Substituted Pyrazoles and Triazoles as Potential Energetic Materials and Oxidizers," *Journal of Materials Chemistry A* 2 (2014): 3200, https://doi.org/10.1039/c3ta15057g.
- 58. Y. Zhang, Q. Sun, K. Xu, J. Song, and F. Zhao, "Review on the Reactivity of 1,1-Diamino-2,2-Dinitroethylene (FOX-7)," *Propellants, Explosives, Pyrotechnics* 41 (2016): 35–52, https://doi.org/10.1002/prep.201500065.
- 59. R. Amrousse, T. Katsumi, N. Azuma, and K. Hori, "Hydroxylammonium Nitrate (HAN)-Based Green Propellant as Alternative Energy Resource for Potential Hydrazine Substitution: From Lab Scale to Pilot Plant Scale-Up," *Combustion and Flame* 176 (2017): 334–348, https://doi.org/10.1016/j.combustflame.2016.11.011.
- 60. X. Zhang, M. Fu, F. Zou, et al., "1,3-Bis(3,4,5-Trifluoro-2,6-Dinitrophenyl)Urea (ZXC-19): A Multifluorine Substituted Propellant With Superior Detonation Performance," *New Journal of Chemistry* 43 (2019): 9623–9627, https://doi.org/10.1039/c9nj01885a.
- 61. T. Jurkat, C. Voigt, S. Kaufmann, et al., "Depletion of Ozone and Reservoir Species of Chlorine and Nitrogen Oxide in the Lower Antarctic Polar Vortex Measured From Aircraft," *Geophysical Research Letters* 44 (2017): 6440–6449, https://doi.org/10.1002/2017GL073270.

- 62. C. E. Williamson, P. J. Neale, S. Hylander, et al., "The Interactive Effects of Stratospheric Ozone Depletion, UV Radiation, and Climate Change on Aquatic Ecosystems," *Photochemical and Photobiological Sciences* 18 (2019): 717–746, https://doi.org/10.1039/C8PP90062K.
- 63. R. Xu, Y. Xie, J. Tian, and L. Chen, "Adsorbable Organic Halogens in Contaminated Water Environment: A Review of Sources and Removal Technologies," *Journal of Cleaner Production* 283 (2021): 124645, https://doi.org/10.1016/j.jclepro.2020.124645.
- 64. P. Kalra, "Impact of Water Toxicity and Acidity on Dynamics of Prey-Predator Aquatic Populations: A Mathematical Model," *Journal of Physics: Conference Series* 1531 (2020): 012081, https://doi.org/10.1088/1742-6596/1531/1/012081.
- 65. M. K. Jeon, S.-W. Kim, and E.-Y. Choi, "Corrosion Behavior of Stainless Steel 316 for Carbon Anode Oxide Reduction Application," *Journal of Nuclear Fuel Cycle and Waste Technology* 18 (2020): 169–177, https://doi.org/10.7733/jnfcwt.2020.18.2.169.
- 66. Y. Liu, W. Fan, and H. Guo, "A Calculation Model for the Overall Process of High Temperature Corrosion Mechanism Induced by Firing Coal With High Chlorine and Sodium Content," *Energy* 205 (2020): 118073, https://doi.org/10.1016/j.energy.2020.118073.
- 67. D. Trache, T. M. Klapötke, L. Maiz, M. Abd-Elghany, and L. T. DeLuca, "Recent Advances in New Oxidizers for Solid Rocket Propulsion," *Green Chemistry* 19 (2017): 4711–4736, https://doi.org/10.1039/c7gc01928a.
- 68. G. K. Williams and T. B. Brill, "Thermal Decomposition of Energetic Materials 67. Hydrazinium Nitroformate (HNF) Rates and Pathways Under Combustion Like Conditions," *Combustion and Flame* 102 (1995): 418–426, https://doi.org/10.1016/0010-2180(94)00283-X.
- 69. J. R. Lovett and N. J. Edison, "Hydrazine Nitroform and Method of Preparation," 3 (1968).
- 70. P. S. Dendage, D. B. Sarwade, S. N. Asthana, and H. Singh, "Hydrazinium Nitroformate (HNF) and HNF Based Propellants: A Review," *Journal of Energetic Materials* 19 (2001): 41–78, https://doi.org/10.1080/07370650108219392.
- 71. V. P. Sinditskii, V. Y. Egorshev, V. V. Serushkin, et al., "Evaluation of Decomposition Kinetics of Energetic Materials in the Combustion Wave," *Thermochimica Acta* 496 (2009): 1–12, https://doi.org/10.1016/j.tca.2009. 07.004.
- 72. A. J. McDonald and R. R. Bennett, "Environmental Impacts From Launching Chemical Rockets," paper presented at Propulsion and Energetics Panel (PEP) 84th Symposium on Environmental Aspects of Rocket and Gun Propulsion, Aalesund, Norway, August 29–September 2, 1994.
- 73. A. S. Cumming, "New Trends in Advanced High Energy Materials," *Journal of Aerospace Technology and Management* 1 (2009): 161–166, https://doi.org/10.5028/jatm.2009.0102161166.
- 74. R. Amrousse, R. Brahmi, Y. Batonneau, and C. Kappenstein, "Thermal and Catalytic Decomposition of H2O2-Ionic Liquid Monopropellant Mixtures on Monolith-Based Catalysts," paper presented at 46th AIAA/ASME/SAE/ASEE Joint Propulsion Conference & Exhibit, Reston, Virigina, 2010, https://doi.org/10.2514/6.2010-6983.
- 75. L. Courthéoux, D. Amariei, S. Rossignol, and C. Kappenstein, "Thermal and Catalytic Decomposition of HNF and HAN Liquid Ionic as Propellants," *Applied Catalysis B* 62 (2006): 217–225, https://doi.org/10.1016/j.apcatb.2005.07.016.
- 76. R. P. van den Berg, P. J. M. Elands, and J. M. Mul, "Monopropellant System," US6755990B1 (2004).
- 77. B. Slettenhaar, J. F. Zevenbergen, and H. J Pasman, "Study on Catalytic Ignition of HNF Based Non Toxic Monopropellants," paper presented at 39th AIAA/ASME/SAE/ASEE Joint Propulsion Conference and Exhibit, Huntsville, 2003.
- 78. H. S. Jadhav, M. B. Talawar, D. D. Dhavale, S. N. Asthana, and V. N. Krishnamurthy, "Synthesis, Characterization and Thermal Behavior of Hydrazinium Nitroformate (HNF) and Its New *N*-Alkyl Substituted Derivatives," *Indian Journal of Chemical Technology* 22 (2005): 187–192.

- 79. D. E. Welch and R. W. Hein, "Process For Producing NitrOFORM," US3491160 (1970).
- 80. A. Langlet, N. V. Latypov, U. Wellmar, P. Goede, and J. Bergman, "Formation of Nitroform in the Nitration of Gem-Dinitro Compounds," *Propellants, Explosives, Pyrotechnics* 29 (2004): 344–348, https://doi.org/10.1002/prep.200400064.
- 81. M. B. Frankel, F. C. Gunderloy Jr, and D. O. I. Woolery, "Production of Trintromethane," US4122124A (1978).
- 82. P. Ding, L. Wen, H. Wang, G. Cheng, C. Lu, and H. Yang, "Preparation of Nitroform From Isopropanol and Study of the Reaction Mechanism," *Industrial & Engineering Chemistry Research* 53 (2014): 10886–10891, https://doi.org/10.1021/ie5011993.
- 83. P. Ding, H. Wang, L. Wen, G. Cheng, C. Lu, and H. Yang, "Studies on Synthetic Technology and Reduced Sensitivity Technology of Hydrazinium Nitroformate," *Industrial & Engineering Chemistry Research* 53 (2014): 13851–13855, https://doi.org/10.1021/ie5023139.
- 84. H. Y. Lu, J. R. Li, D. L. Yang, Q. Zhang, and D. X. Shi, "A Novel Synthesis of Nitroform by the Nitrolysis of Cucurbituril," *Chinese Chemical Letters* 26 (2015): 365–368, https://doi.org/10.1016/j.cclet.2014.12.
- 85. C. Yan, P. Ding, H. Yang, C. Lu, and G. Cheng, "New Synthetic Route of Nitroform (NF) From Acetylacetone and Study of the Reaction Mechanism," *Industrial & Engineering Chemistry Research* 55 (2016): 11029–11034, https://doi.org/10.1021/acs.iecr.6b02049.
- 86. F. Raschig, "Production of Hydrazin" (1909).
- 87. O. Seuffert, "hwe E. Manufacture of Hydrazine" (1934).
- 88. J. Schirmann and B. P. Hydrazine, *Ullmann's Encyclopedia of Industrial Chemistry* (Wiley, 2001), https://doi.org/10.1002/14356007.a13 177.
- 89. H. Hayashi, "Hydrazine Synthesis by a Catalytic Oxidation Process," *Catalysis Reviews* 32 (1990): 229–277, https://doi.org/10.1080/01614949009351352.
- 90. W. H. M. Veltmans and F. J. M. Wierckx, "Process for the Production of Crystalline Energetic Materials," US6841016B1 (2005).
- 91. H. F. R. Schöyer, A. J. Schnorhk, P. Korting, et al., "Development of Hydrazinium Nitroformate Based Solid Propellants," paper presented at 31st Joint Propulsion Conference and Exhibit, San Diego, CA, July 10–12, 1995, https://doi.org/10.2514/6.1995-2864.
- 92. H. S. Jadhav, B. Talawar, D. D. Dhavale, N. Asthana, and V. N. Krishnamurthy, "Synthesis, Characterization and Thermal Behavior of Hydrazinium Nitroformate (HNF) and Its New *N*-Alkyl Substituted Derivatives," *Indian Journal of Chemical Technology* 12 (2005): 187–192.
- 93. L. Du, S. Jin, Y. Liu, et al., "Theoretical Study on the Weak Interaction and Energy Performance of Nitroformate Salts and Nitroformate-Based Propellant Formulations," *Journal of Molecular Modeling* 25 (2019): 285, https://doi.org/10.1007/s00894-019-4164-7.
- 94. B. Dickens, "The Crystal Structure of Hydrazine Nitroform  $[N_2H_5+C(NO_2)_3-]$ ," Chemical Communications 5 (1967): 246–247, https://doi.org/10.1039/C19670000246.
- 95. N. V. Podberezskaya, V. P. Doronina, V. V. Bakakin, and I. I. Yakovlev, "Crystal Structure of Hexamminenickel(II) Nitroformate," *Zhurnal Strukturnoi Khimii* 25 (1984): 182–185.
- 96. X. Zhang, Y. Liu, F. Wang, and X. Gong, "A Theoretical Study on the Structure, Intramolecular Interactions, and Detonation Performance of Hydrazinium Dinitramide," *Chemistry—An Asian Journal* 9 (2014): 229–236, https://doi.org/10.1002/asia.201300842.
- 97. E. Espinosa, E. Molins, and C. Lecomte, "Hydrogen Bond Strengths Revealed by Topological Analyses of Experimentally Observed Electron Densities," *Chemical Physics Letters* 285 (1998): 170–173, https://doi.org/10.1016/S0009-2614(98)00036-0.
- 98. H. Schoeyer, A. Schnorhk, P. A. O. G. Korting, et al., "Development of Hydrazinium Nitroformate Based Solid Propellants." paper presented

- at 31st Joint Propulsion Conference and Exhibit, 1995, https://doi.org/10. 2514/6.1995-2864.
- 99. P. M. Jadhav, S. Radhakrishnan, V. D. Ghule, and R. K. Pandey, "Energetic Salts From Nitroformate Ion," *Journal of Molecular Modeling* 21 (2015): 134, https://doi.org/10.1007/s00894-015-2682-5.
- 100. E. W. Schmidt and W. Eckart. *Hydrazine and Its Derivatives: Preparation, Properties, Applications*, 2nd ed. (Wiley, 2001).
- 101. D. M. Badgujar, M. B. Talawar, S. N. Asthana, and P. P. Mahulikar, "Advances in Science and Technology of Modern Energetic Materials: An Overview," *Journal of Hazardous Materials* 151 (2008): 289–305, https://doi.org/10.1016/j.jhazmat.2007.10.039.
- 102. "Energetic Materials: Analysis, Diagnostics and Testing," paper presented at 31st International Annual Conference of ICT, 2000.
- 103. A. Majumder and Z. K. Nagy, "Prediction and Control of Crystal Shape Distribution in the Presence of Crystal Growth Modifiers," *Chemical Engineering Science* 101 (2013): 593–602, https://doi.org/10.1016/j.ces. 2013.07.017.
- 104. F. Salvatori and M. Mazzotti, "Manipulation of Particle Morphology by Crystallization, Milling, and Heating Cycles: Experimental Characterization," *Industrial & Engineering Chemistry Research* 57 (2018): 15522–15533, https://doi.org/10.1021/acs.iecr.8b03349.
- 105. L. M. Belca, A. Ručigaj, D. Teslič, and M. Krajnc, "The Use of Ultrasound in the Crystallization Process of an Active Pharmaceutical Ingredient," *Ultrasonics Sonochemistry* 58 (2019): 104642, https://doi.org/10.1016/j.ultsonch.2019.104642.
- 106. J. Athar, M. Ghosh, P. S. Dendage, R. S. Damse, and A. K. Sikder, "Nanocomposites: An Ideal Coating Material to Reduce the Sensitivity of Hydrazinium Nitroformate (HNF)," *Propellants, Explosives, Pyrotechnics* 35 (2010): 153–158, https://doi.org/10.1002/prep.200900024.
- 107. P. W. Cains, P. D. Martin, and C. J. Price, "The Use of Ultrasound in Industrial Chemical Synthesis and Crystallization. 1. Applications to Synthetic Chemistry," *Organic Process Research & Development* 2 (1998): 34–48, https://doi.org/10.1021/op9700340.
- 108. A. Davenas, G. Jacob, Y. Longevialle, and C. Perut, "Energetic Compounds for Future Applications," in *2nd International Conference on Green Propellants for Cagliari*, ed. A. Wilson (2004).
- 109. H. F. R. Schoyer, W. H. M. Welland-Veltmans, J. Louwers, et al., "Overview of the Development of Hydrazinium Nitroformate," *Journal of Propulsion and Power* 18 (2002): 131–137, https://doi.org/10.2514/2.5908.
- 110. J. Louwers and A. Van Der Heijden, "Hydrazinium Nitroformate," US6572717B1 (2003).
- 111. B. Asgharian and O. R. Moss, "Particle Suspension in a Rotating Drum Chamber When the Influence of Gravity and Rotation are Both Significant," *Aerosol Science and Technology* 17 (1992): 263–277, https://doi.org/10.1080/02786829208959575.
- 112. H. F. R. Schoeyer, A. J. Schnorhk, P. Korting, et al., "High-Performance Propellants Based on Hydrazinium Nitroformate," *Journal of Propulsion and Power* 11 (1995): 856–869, https://doi.org/10.2514/3.23 911.
- 113. H. Schoeyer, P. Korting, W. Veltmans, et al. "An Overview of the Development of HNF and HNF-Based Propellants," paper presented at 36th AIAA/ASME/SAE/ASEE Joint Propulsion Conference and Exhibit, Reston, VA, 2000, https://doi.org/10.2514/6.2000-3184.
- 114. G. V. Belov, A. N. Kitin, and N. I. Shustova, "Conditions for Initiating Explosive Transformation in Phlegmatized HMX Samples on Impact With Low-Velocity Indenters With a Spherical End," *Combustion, Explosion, and Shock Waves* 56 (2020): 100–105, https://doi.org/10.1134/S0010508220010128.
- 115. A. Elbeih, M. Abd-Elghany, and T. Elshenawy, "Application of Vacuum Stability Test to Determine Thermal Decomposition Kinetics of Nitramines Bonded by Polyurethane Matrix," *Acta Astronautica* 132 (2017): 124–130, https://doi.org/10.1016/j.actaastro.2016.12.024.

- 116. G. Gadiot, J. M. Mul, P. J. van Lit, and P. Körting, "Hydrazinium Nitroformate and Its Use as Oxidizer in High Performance Solid Propellants," paper presented at Propulsion and Energetics Panel (PEP) 84th Symposium on Environmental Aspects of Rocket and Gun Propulsion, Aalesund, Norway, August 29–September 2, 1994.
- 117. G. Gadiot, J. M. Mul, J. J. Meulenbrugge, P. Korting, A. J. Schnorkh, and H. F. R. Schöyer, "New Solid Propellants Based on Energetic Binders and HNF," *Acta Astronautica* 29 (1993): 771–779, https://doi.org/10.1016/0094-5765(93)90158-S.
- 118. M. A. Bohn, "Thermal Stability of HNF Investigated by Mass Loss and Heat Generation in the Temperature Range 50°C to 80°C and Lifetime Predictions," paper presented at 36th International Annual Conference of ICT and the 32nd International Pyrotechnics Seminar, 2005.
- 119. P. S. Dendage, D. B. Sarwade, A. B. Mandale, and S. N. Asthana, "Characterization and Thermal Analysis of Hydrazinium Nitroformate (HNF)," *Journal of Energetic Materials* 21 (2003): 167–183, https://doi.org/10.1080/716100384.
- 120. W. P. C. De Klerk, C. Popescu, and A. E. D. M. van der Heijden, "Study on the Decomposition Kinetics of Fox-7 and HNF," *Journal of Thermal Analysis and Calorimetry* 72 (2003): 955–966.
- 121. L. Courtheoux, D. Amariei, S. Rossignol, C. Kappenstein, N. Pillet, and M. Ford, "Thermal and Catalytic Decomposition of HNF and HAN-Based Propellants," European Space Agency, (Special Publication) ESA SP 557 (2004): 18.
- 122. K. Farhat, C. Kappenstein, and Y. Batonneau, "Thermal and Catalytic Decomposition of AN-, ADN and HNF-Based Ionic Monopropellants," paper presented at 44th AIAA/ASME/SAE/ASEE Joint Propulsion Conference & Exhibit, Reston, Virigina: American Institute of Aeronautics and Astronautics; 2008, https://doi.org/10.2514/6.2008-4938.
- 123. V. G. Kiselev and N. P. Gritsan, "Theoretical Study of the Primary Processes in the Thermal Decomposition of Hydrazinium Nitroformate," *Journal of Physical Chemistry A* 113 (2009): 11067–11074, https://doi.org/10.1021/jp906853e.
- 124. V. P. Sinditskii, V. Y. Egorshev, P. Astori, V. V. Serushkin, and A. I. Levchenkov, "Combustion Peculiarities of Chlorine-Free Oxidizers Adn And Hnf," *Proceedings of 3rd International High Energy Materials Conference and Exhibiton* 8 (1971): 489–494, https://doi.org/10.1021/acs.joc.6b00134.
- 125. V. P. Sinditskii, V. Y. Egorshev, V. V. Serushkin, and A. I. Levshenkov, "Chemical Peculiarities of Combustion of Solid Propellant Oxidizers" (2002).
- 126. O. Dragomir, M. Tummers, D. Roekaerts, and A. Heijden, "Flame Structure Analysis of Hydrazinium Nitroformate (HNF) By Using Laser Doppler Anemometry" (2005).
- 127. O. E. Dragomir, M. J. Tummers, E. H. van Veen, A. van der Heijden, and D. Roekaerts, "Experimental Investigation of the HNF Flame Structure," *Combustion and Flame* 153 (2008): 149–160, https://doi.org/10.1016/j.combustflame.2007.10.009.
- 128. T. B. Brill, H. Arisawa, P. J. Brush, P. E. Gongwer, and G. K. Williams, "Surface Chemistry of Burning Explosives and Propellants," *Journal of Physical Chemistry* 99 (1995): 1384–1392, https://doi.org/10.1021/j100005a005.
- 129. J. Louwers, Combustion and Decomposition of Hydrazinium Nitroformate (HNF) and HNF Propellants (TU Delft, 2000).
- 130. L. T. DeLuca and A. Annovazzi, "Survey of Burning Rate Measurements in Small Solid Rocket Motors," *FirePhysChem* 4 (2024): 146–165, https://doi.org/10.1016/j.fpc.2023.11.004.
- 131. S. Mankan and L. Bose, "Review on Past, Present and Future Rocket Propulsion Technologies," *International Journal of Scientific Research in Engineering and Management* 8 (2024): 1–12.
- 132. S. Prarthana and M. Malaya Kumar Biswal, "A Short Review on ISRO Rocket Engines," *Acceleron Aerospace Journal* 1 (2023): 95–100, https://doi.org/10.61359/11.2106-2320.

- 133. M. S. Kellison, K. L. Gee, W. L. Coyle, M. C. Anderson, L. T. Mathews, and G. W Hart, "Aeroacoustical Analyses From the Space Launch System Artemis-I Mission," 30th AIAA/CEAS Aeroacoustics Conference 2024, American Institute of Aeronautics and Astronautics Inc, AIAA; 2024, https://doi.org/10.2514/6.2024-3033.
- 134. W. Welland, A. van der Heijden, S. Cianfanelli, and L. Batenburg, "Improvement of HNF and Propellant Characteristics of HNF-Based Composite Propellants," 43rd AIAA/ASME/SAE/ASEE Joint Propulsion Conference & Exhibit, American Institute of Aeronautics and Astronautics, 2007, https://doi.org/10.2514/6.2007-5764.
- 135. J. Mul, G. Gadiot, J. Meulenbrugge, P. Korting, A.-J. Schnorhk, and H. Schoyer. "New Solid Propellants Based on Energetic Binders and HNF." 28th Joint Propulsion Conference and Exhibit, Reston, Virigina: American Institute of Aeronautics and Astronautics; 1992, https://doi.org/10.2514/6.1992-3627.
- 136. H. F. R. Schoyer, P. Korting, and J. M Mul, US4938814, 1990.
- 137. J. Mul, P. Korting, and H. Schoyer. "Search for New Storable High Performance Propellants." 24th Joint Propulsion Conference, Reston, Virigina: American Institute of Aeronautics and Astronautics; 1988, https://doi.org/10.2514/6.1988-3354.
- 138. Y. Ou, B. Chen, H. Yan, H. Jia, J. Li, and S. Dong, "Development of Energetic Additives for Propellants in China," *Journal of Propulsion and Power* 11 (1995): 838–847, https://doi.org/10.2514/3.23909.
- 139. L. Zhang, Q. Lin, B. Cheng, P. Wang, M. Lu, and Q. Lin, "Effect of Hexanitroethane (HNE) and Hydrazinium Nitroformate (HNF) on Energy Characteristics of Composite Solid Propellants," *FirePhysChem* 1 (2021): 116–122. https://doi.org/10.1016/j.fpc.2021.05.003.
- 140. A. van der Heijden, H. Keizers, L. van Vliet, et al., "Ballistic Properties of HNF/Al/HTPB Based Propellants," Proceedings of the 32nd International Annual Conference of ICT, 2001.
- 141. W. Welland, A. van der Heijden, S. Cianfanelli, and L. Batenburg, "Improvement of HNF and Propellant Characteristics of HNF-Based Composite Propellants," 43rd AIAA/ASME/SAE/ASEE Joint Propulsion Conference & Exhibit, Reston, Virigina: American Institute of Aeronautics and Astronautics; 2007, https://doi.org/10.2514/6.2007-5764.
- 142. M. J. Tummers, A. van der Heijden, and E. H. van Veen, "Selection of Burning Rate Modifiers for Hydrazinium Nitroformate," *Combustion and Flame* 159 (2012): 882–886, https://doi.org/10.1016/j.combustflame. 2011.08.010.
- 143. G. M. Low and V. E Haury. US3708359. US Patent, (1973).
- 144. G. Da Silva, S. C. Rufino, and K. Iha, "Green Propellants—Oxidizers," *Journal of Aerospace Technology and Management* 5 (2013): 139–144, https://doi.org/10.5028/jatm.v5i2.229.
- 145. V. E. Haury, "Hydrazinumnitroformate Propellant Stabelized With Ntroguandine," US3658608 (1972).
- 146. T. M. Deppert, D. R. Smith, and C. Shanholtz, "Methods To Desenstize Hydrazinium Nitroformate," US 9505666 B2 (2016).